

Effect of alpha 2,6 Sialylation and Ionizing Radiation on Integrin-mediated Cell
Adhesion and Cell Cycle Arrest

A dissertation presented to
the faculty of
the College of Arts and Sciences of Ohio University

In partial fulfillment
of the requirements for the degree
Doctor of Philosophy

Ye Yuan

December 2016

© 2016 Ye Yuan. All Rights Reserved.

This dissertation titled
Effect of alpha 2,6 Sialylation and Ionizing Radiation on Integrin-mediated Cell
Adhesion and Cell Cycle Arrest

by

YE YUAN

has been approved for
the Department of Chemistry and Biochemistry
and the College of Arts and Sciences by

Shiyong Wu

Professor of Chemistry and Biochemistry

Robert Frank

Dean, College of Arts and Sciences

ABSTRACT

YUAN, YE, Ph.D., December 2016, Chemistry

Effect of alpha 2,6 Sialylation and Ionizing Radiation on Integrin-mediated Cell Adhesion and Cell Cycle Arrest

Director of Dissertation: Shiyong Wu

Cell adhesion is an important early step of cancer metastasis, yet the roles of sialylation in regulating integrin-mediated breast cancer cell adhesion in comparison to migration and invasion are not well-understood. The role of sialylation on $\alpha 5\beta 1$ and $\alpha 2\beta 1$ integrins in the regulation of adhesion between breast cancer cells and extracellular matrix (ECM) was studied. Our data showed that $\alpha 2$, $\alpha 5$ and $\beta 1$ integrins had considerable $\alpha 2,6$ sialylation on MDA-MB-231 cells, whereas signals from MCF-7 cells were undetectable. Cleavage of $\alpha 2,6$ sialylation increased adhesion of MDA-MB-231 cells to ECM, while adhesion of MCF-7 cells was unaffected, consistent with the latter's lack of endogenous $\alpha 2,6$ sialylated surface integrins. Neither surface expression of $\alpha 2\beta 1$ and $\alpha 5\beta 1$ integrins, nor activated $\beta 1$ integrin, changed in MDA-MB-231 cells after sialidase treatment. However, sialidase treatment did not have significant impact on migration or invasion of MDA-MB-231 cells.

Integrins not only play an important role in adhesion of cancer cells, but also have a direct connection with ionizing radiation-induced atherosclerosis, which is an adverse effect observed after radiotherapy. However, minimal attention has been given to monocytes/macrophages, which are exposed to the

radiation at the same time. Under flow conditions using a parallel plate flow chamber to mimic physiological shear stress, we demonstrate here that the avidity between very late antigen-4 (VLA-4) of RAW264.7 cells and its ligand vascular cell adhesion molecule-1 (VCAM-1), was increased after low dose (0.5 Gy), but was reduced after higher dose (5 Gy) treatment of ionizing radiation. Treating the cells with free radical scavenger N-acetyl-L-cysteine reduced the avidity between RAW264.7 cells and VCAM-1 to a similar level. These results suggest that ionizing radiation regulates adhesive interactions between VLA-4 and VCAM-1, and that reactive oxygen species might function as a regulator, for this increased adhesiveness but with altered expression of integrin not play a major role.

In addition to regulation of cell adhesion, ionizing radiation (IR) is known to induce cell cycle arrest which correlates with cell proliferation and cell death. Recent studies connect IR with endoplasmic reticulum (ER) stress, leading to activation of PKR-like endoplasmic reticulum kinase (PERK) and subsequent phosphorylation of eukaryotic translation initiation factor 2 α (eIF2 α). However, the contribution of PERK and eIF2 α phosphorylation in IR-induced G₂/M arrest is incompletely understood. Here we report that IR-induced eIF2 α phosphorylation was predominantly mediated by PERK and IR-induced G₂/M arrest was blunted after totally abolishing eIF2 α phosphorylation. Our results reveal that basal level of eIF2 α phosphorylation is indispensable to maintain G₂/M arrest in response to IR.

DEDICATION

This work is dedicated to my parents

Thank you for supporting me throughout my life

and

My friend ShiTao who has left us too soon

ACKNOWLEDGMENTS

Here I want take this opportunity to thank people who generously helped me during my PhD study at Ohio University. First I want to express my sincere appreciation to my advisor, Dr. Shiyong Wu. His enthusiasm and passion for biochemistry has established an example for our lab and kept motivating me in past years. I am very grateful for his constant encouragement and professional support.

My thanks also go out to my dissertation committee, Dr. Michael Held, Dr. Hao Chen and Dr. Monica Burdick. I appreciate their valuable advice on my proposal and assistance in a timely manner despite their busy schedule. I am grateful to Dr. Monica Burdick for her comprehensive guidance and careful revision in the project of integrin sialylation.

My appreciation extends to my excellent labmates and visiting students: Dr. Lingying Tong, Dr. Oliver L. Carpenter, Dr. Qiong Wu, Dr. Huiwen Cheng, Dr. Yi Liao, Dr. Jianguo Feng, Huizhi Zhao, Guangyu Fan, Siqi Shen and Curran Rhodes. It was always a pleasure to have a discussion with them. Their professional assistance and companionship made my life and study enjoyable. The experience of working with them is a real treasure in my life.

In addition, I would like to thank the Department of Chemistry and Biochemistry for offering me the great opportunity to be a teaching assistant. Thanks to support from Dr. Frazier Nyasulu, Aaron Dillon and Leslie Scripp, I had a great time teaching undergraduate students in labs. I appreciate professional

assistance from Lori Abdella and Marlene Jenkins. I also thank Michelle Pate for assistance in using the FACS Aria.

Finally, I want to thank my parents and old friends for their constant support in this limited space. They witnessed my progress and will be always there no matter where I go.

TABLE OF CONTENTS

	Page
Abstract	3
Dedication	5
Acknowledgments	6
List of Figures	9
List of Abbreviations	11
Chapter 1 : Introduction	13
Integrins and Integrin-mediated Cell Adhesion	13
Radiation Therapy.....	16
Endoplasmic Reticulum Stress/Unfolded Protein Response.....	21
Chapter 2 : Effect of alpha 2,6 Sialylation on Integrin-mediated Adhesion of Breast Cancer Cells to Fibronectin and Collagen IV.....	23
Introduction	23
Materials and Methods.....	24
Results.....	29
Discussion	44
Chapter 3 : The Role of ROS in Ionizing Radiation-induced VLA-4 Mediated Adhesion of RAW264.7 Cells to VCAM-1 Under Flow Conditions.....	47
Introduction	47
Materials and Methods.....	49
Results.....	51
Discussion	58
Chapter 4 : The Roles of PERK and eIF2 α Phosphorylation in Ionizing Radiation-induced G2/M Arrest.....	62
Introduction	62
Materials and Methods.....	64
Results.....	67
Discussion	78
Chapter 5 : Future Directions.....	82
References	84

LIST OF FIGURES

	Page
<i>Figure 1.1</i> IR-induced DNA damage in cells.....	17
<i>Figure 2.1</i> Monoclonal antibody blockade assay.....	31
<i>Figure 2.2</i> Sialylation of relevant integrins on MDA-MB-231 and MCF-7 cells. ..	32
<i>Figure 2.3</i> Effect of sialidase on adhesion of MDA-MB-231 cells, MCF-7 cells and HT-29 cells to ECM.	35
<i>Figure 2.4</i> Detection of sialic acid cleavage on MDA-MB-231 and MCF-7 cells by flow cytometry after sialidase treatment.	39
<i>Figure 2.5</i> Surface expression of relevant integrins on MDA-MB-231 and MCF-7 cells after sialidase treatment.	42
<i>Figure 2.6</i> Effect of sialidase on migration and invasion of MDA-MB-231 cells..	44
<i>Figure 3.1</i> Expression of $\alpha 4$ and $\beta 1$ integrins in RAW264.7 cells after ionizing radiation.....	52
<i>Figure 3.2</i> Adhesion of irradiated RAW264.7 cells to VCAM-1 under flow conditions.	55
<i>Figure 3.3</i> Effect of L-NAC on VLA-4 mediated adhesion of RAW264.7 cells under flow conditions.....	56
<i>Figure 3.4</i> H ₂ O ₂ regulates avidity of VLA-4 in RAW264.7 cells under flow conditions.	58
<i>Figure 4.1</i> eIF2 α phosphorylation at 1 h, 6 h and 24 h following IR was measured by Western blot.....	67

	10
<i>Figure 4.2</i> Cell growth was measured at 24 h and 48 h post irradiation.	68
<i>Figure 4.3</i> Cell death was evaluated by Annexin V-FITC and PI double staining at 72 h after IR.....	69
<i>Figure 4.4</i> IR-induced G ₂ /M arrest in MEFs. MEF ^{WT} , MEF ^{PERK^{-/-}} and MEF ^{A/A} cells were irradiated with 10 Gy.	73
<i>Figure 4.5</i> Cells were irradiated with 10 Gy after serum starvation for 24 h.	75
<i>Figure 4.6</i> Effect of KU55933 on IR-induced G ₂ /M arrest in MEFs.....	77
<i>Figure 4.7</i> MEFs were treated with hydroxyurea (0.5 mM) for 24 h.....	80
<i>Figure 4.8</i> A proposed model for the roles of PERK and eIF2α phosphorylation in the regulation of IR-induced G ₂ /M arrest.	81
<i>Figure 5.1</i> Oxygen consumption rate (OCR) of MEFs.	83

LIST OF ABBREVIATIONS

ATF4	activating transcription factor 4
ATF6	activating transcription factor 6
ATM	ataxia telangiectasia mutated
BSA	bovine serum albumin
CHOP	C/EBP homologous protein
CDK	cyclin-dependent kinase
DSBs	DNA double-strand breaks
DMEM	Dulbecco's modified eagle medium
ER	endoplasmic reticulum
EGF	epidermal growth factor
eIF2 α	eukaryotic initiation factor 2 α
ECM	extracellular matrix
ERK	extracellular signal–regulated kinase
FBS	fetal bovine serum
FITC	fluorescein isothiocyanate
FAK	focal adhesion kinase
GCN2	general control nonderepressible 2
GRP	glucose-regulated protein
HRP	horse radish peroxidase
IRE1	inositol-requiring enzyme 1
ICAM-1	intercellular adhesion molecule-1
IR	ionizing radiation
MnSOD	manganese superoxide dismutase
MIDAS	metal ion dependent adhesion site
MEM	minimal essential medium
MAPK	mitogen-activated protein kinase
MEF	mouse embryonic fibroblast

MRN	MRE11-RAD50-NBS1
L-NAC	N-Acetyl-L-cysteine
NEAA	non-essential amino acids
OxLDL	oxidized low-density lipoprotein
OCR	oxygen consumption rate
PBS	phosphate buffered saline
PERK	PKR-like ER kinase
PECAM-1	platelet endothelial cell adhesion molecule-1
PSI	plexin-semaphorin-integrin
PI	propidium iodide
RNS	reactive nitrogen species
ROS	reactive oxygen species
SNA	sambucus nigra lectin
SSBs	single strand breaks
SDS-PAGE	sodium dodecyl sulfate polyacrylamide gel electrophoresis
TBS	Tris-buffered saline
TBS-T	Tris-buffered saline with Tween
UPR	unfolded protein response
VCAM-1	vascular cell adhesion molecule 1
VLA-4	very late antigen-4
vWF	von Willebrand factor
XBP-1	X box protein-1

CHAPTER 1 : INTRODUCTION

Integrins and Integrin-mediated Cell Adhesion

Integrins, first identified in 1986, are transmembrane proteins which are originally known to connect cytoskeleton with extracellular matrix (ECM) [1].

Further it is known that there are different ways to combine 18 α with 8 β subunits in vertebrates so that 24 heterodimers are formed [2, 3].

The major parts of integrins are extracellular domains. In most cases, α subunits (~1000 amino acids) are slightly larger than β subunits (~750 amino acids). In addition to β -propeller, thigh and calf domains, half of α chains have α -I domains which are similar to the β chains. For β subunits, they also contain plexin-semaphorin-integrin (PSI) domains and epidermal growth factor (EGF) modules in the extracellular parts [4, 5]. The binding site of divalent cations Mg^{2+} in I domain is referred to as metal ion dependent adhesion sites (MIDAS), which is crucial in ligand binding [6]. Compared to the bulky extracellular domains, cytoplasmic tails of integrins are very short with exception of $\beta 4$ [7].

Integrins can be classified based on their ligands [2]. For example, integrins which recognize the RGD sequence are known as RGD receptors (e.g., $\alpha V\beta 3$, $\alpha V\beta 5$, $\alpha V\beta 6$, $\alpha V\beta 8$, $\alpha 5\beta 1$, $\alpha 8\beta 1$). Though only about 30% of integrins bind to RGD peptides, it is very important because RGD peptides are in classic ligands fibronectin, fibrinogen and vitronectin [8, 9]. Similarly, collagen receptors such as $\alpha 1\beta 1$, $\alpha 2\beta 1$, $\alpha 10\beta 1$, $\alpha 11\beta 1$ integrins are able to recognize the triple

helical GFOGER sequence [10]. There are also laminin receptors (e.g., $\alpha 2\beta 1$, $\alpha 6\beta 1$) and leukocyte-specific receptors (e.g., $\alpha L\beta 2$, $\alpha M\beta 2$) [2].

Integrins are found widely in cells and play important roles in mediating cell adhesion, migration and signal transduction. After adhesion between integrins and ECM is secured, cells gain necessary traction for migration [11]. The equilibrium of adhesion formation and release regulates the speed of migration. For signal transduction, on the one hand, the ligand affinity of integrins is regulated by inside-out signals, which induce changes of conformation [12]. A well-studied mechanism of integrin activation requires a signaling molecule, talin, to attach to the cytoplasmic tail of the β subunit via the phosphotyrosine binding-like domain. This is followed by separation of α and β transmembrane domains [13-15]. Eventually, a higher affinity state of integrins is achieved after a series of conformational changes of extracellular domains. Under the regulation of inside-out signaling, cells like leukocytes do not aggregate and adhere to intact endothelium unless signals from other receptors (e.g., T-cell receptor, selectin) activate integrins, leading to firm integrin-mediated adhesion [16, 17]. On the other hand, activated integrins also regulate a variety of intracellular signals, which is known as outside-in signaling [18]. This process is complex due to availability of different signaling pathways in specific cell types. ECM attachment to integrin may result in cytoskeletal rearrangements of cells within 1 hour to prepare for migration and cause different gene expression after longer attachment. A wide range of pathways are involved in outside-in signaling either

directly or indirectly. For instance, ECM attachment activates focal adhesion kinase (FAK), an important part of focal adhesion complex, resulting in Src activation [19] [20]. The activated FAK-Src complex is essential for mitogen-activated protein kinase (MAPK) activation because it regulates phosphorylation of MEK1 [21]. Integrins also influence cell responses to stimulants. Upon stimulation of growth factors, cell adhesion mediated by $\alpha 5\beta 1$ strengthens activation of extracellular signal-regulated kinase (ERK), which also affects expression of cyclin D1 [22]. Therefore, outside-in signaling regulates more than cell adhesion and motility.

Due to the important physiological roles of integrins in cell adhesion and migration, it is not difficult to understand they are also involved in cancer progression [23]. One typical example is melanoma expressing $\alpha V\beta 3$, $\alpha 5\beta 1$ and $\alpha 4\beta 1$ integrins [24-26]. When cancer cells get chances to adhere to endothelium, cancer cells may migrate through the layer of endothelial cells, which is known as extravasation [27]. Melanoma cells with higher metastatic potential enhance transendothelial migration by strengthened interactions between vascular cell adhesion molecule 1 (VCAM-1) by $\alpha 4\beta 1$ (Very Late Antigen-4, VLA-4) [28]. The contribution of $\alpha 4\beta 1$ integrin to extravasation is also confirmed under low flow conditions [29].

Radiation Therapy

Radiation therapy is widely known as a cost-effective way for cancer treatment. According to the past reports, it is estimated that 3.5 million patients benefited from radiation therapy in terms of the rates of cure while equal amount of patients achieved palliative relief. In addition, although the indication of radiation therapy is undergoing a change, approximately half of cancer patients are in need of radiation therapy [30-32].

The major mechanism through which radiation therapy works is by causing DNA damage. By delivering strong energy to the cells, it not only causes DNA double-strand breaks (DSBs) and single strand breaks (SSBs) directly but also generates base modification [33, 34]. Earlier studies show a single dose of 1 Gy is able to cause 35 DSBs and 1000 SSBs in a cell [35, 36]. This damage to DNA can be detected using the comet assay (Fig 1.1). Irradiated cells must then pause their cell cycle to repair DNA damage. Among different types of IR-induced DNA damage, DSBs are considered to be the primary mechanism to kill cells, though the cell death is not limited to apoptosis [37, 38]. In addition to direct effects on DNA strands, IR leads to prolonged damage to cell by inducing reactive oxygen species (ROS) [39, 40]. These original ROS is from radiolysis of water in the cell, including H_2O_2 , $\cdot\text{OH}$, and $\text{O}\cdot_2^-$. A well-known oxidation of bases in DNA is 8-hydroxyguanine [41], which is a daily physiological lesion, but can be spurred by IR-induced ROS. In addition to ROS derived from radiolysis, IR alters intracellular ROS by inducing mitochondria dysfunction [42]. Mitochondrion is the

site of oxidation phosphorylation and thus the normal source of intracellular ROS [43, 44]. IR stimulates the electron transport chain and increases production of ROS [45].

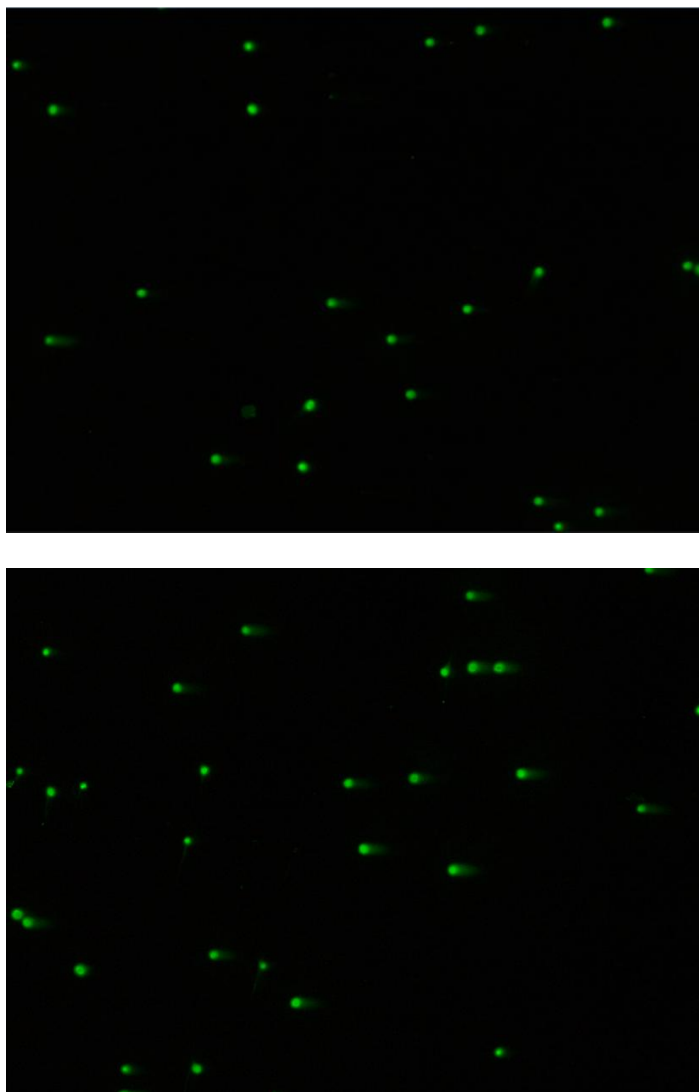


Figure 1.1 IR-induced DNA damage in cells. Wild type mouse embryonic fibroblasts (MEFs) were treated with ionizing radiation (10 Gy). DNA damage at 1 h postirradiation was detected by the comet assay in neutral conditions. Upper panel: MEF without IR. Lower panel: MEF after IR.

Radiation therapy has advantages to treat localized tumors and is frequently combined with chemotherapy and surgery to maximize the effect of treatment. With the development of techniques in the past years, radiation therapy has been applied to a variety of types of cancer, including but not limited to bladder cancer [46], prostate cancer [47], colorectal cancer [48], breast cancer [49], hepatocellular carcinoma [50], lung cancer [51], pancreatic cancer [52], and cervical cancer [53]. In addition, radiation therapy can also treat non-cancerous conditions, such as Cushing's disease and Dupuytren's disease [54, 55].

Given that cancer may recur, adjuvant radiation therapy is frequently used after surgery to prolong the disease-free period. One study showed by collecting data from 13 trials included 12,075 patients, adjuvant radiation therapy significantly improved relapse-free survival of stage I seminoma patients after orchiectomy, though overall survival did not change [56]. The effect of radiation therapy on inhibiting recurrence of triple-negative breast cancer after surgery has been reported by different researchers. A meta-analysis of triple-negative breast cancer showed adjuvant radiation therapy could raise overall survival of patients younger than 40 and patients with late-stage breast cancer [57]. Another group showed that disease-free survival could also be increased in patients with T1-T2 cancer. Both locoregional recurrence-free survival and disease-free survival were improved by radiation therapy in patients with T3-T4 cancer [58].

In treating some types of cancer, the best outcome is found when chemotherapy and radiation therapy are used together. For instance, although

radiation therapy cannot still replace radical surgery for bladder cancer now, the combination of drugs and radiation therapy has created possibilities to preserve patients' organs, which is important to improve quality of life [58, 59].

Radiation therapy is also used to manage cancer metastasis.

Postoperative stereotactic body radiation therapy has been shown to control spinal metastasis, which is very common among cancer patients [60]. For patients with bone metastasis, successful pain management may significantly improve quality of life. Either a single dose of 8 Gy or multiple fractions of 20 Gy was used to provide palliation to late-stage cancer patients with bone metastasis [61].

Advances in techniques and facilities of radiation therapy have significantly reduced the dose that healthy tissue and essential organs are exposed to in recent years. However, ionizing radiation is still a double-edged sword depending on the dose of radiation absorbed by normal tissue during treatment. Clinical practice has confirmed common adverse effects, including edema [62], dermatitis [63], osteonecrosis [64], nausea, vomiting [65], fatigue [66] and etc. Besides these short-term effects, researchers are more concerned with long-term effects on essential organs.

Dating back to the 1970s, researchers reported the correlation between ionizing radiation and heart disease [67]. Today, the evidence has accumulated that a clinical dose of ionizing radiation leads to cardiovascular diseases. According to a study of registered breast cancer patients from 1973 to 2001,

mortality from heart disease of the patients who received radiation therapy was seen to increase after 10-20 years [68]. When radiation therapy is utilized to treat breast cancer, lung cancer, esophageal cancer or other tumors within the thoracic region, the impact on heart and vessels become the limiting factor for dose prescription [69, 70]. In patients with left-sided breast cancer, the dose received by heart and coronary artery was shown to be much greater compared with right-sided patients [71].

Atherosclerosis is a common and important heart disease induced by IR. Previous studies showed that high dose of IR (14 Gy) promoted development of atherosclerosis in ApoE $-/-$ mice [72]. No significant systemic inflammatory markers were increased postirradiation, but the atherosclerotic lesions were infiltrated by macrophages. In addition, fractionated IR (20 X 2 Gy) also resulted in atherosclerotic lesions, although the effect was delayed compared to a single high dose of 14 Gy [73]. A recent study showed that a dose as low as 0.3 Gy promoted atherogenesis in ApoE $-/-$ mice, even if when the low dose was delivered over the duration of 300 days [74]. In fact, the association between low-dose radiation (less than 0.5 Gy) and the long-term risk of cardiovascular diseases has raised people's concern [75][76]. The mechanism of IR-induced atherosclerosis is complicated and remains unclear because there are many contributing factors, which involve oxidative stress, endothelial inflammation, DNA damage, cell apoptosis and senescence [77][78].

Endoplasmic Reticulum Stress/Unfolded Protein Response

Endoplasmic reticulum (ER) is the site for protein folding and transport in eukaryotic cells [79-81]. It also serves as the major stock of calcium in the cell due to active transport by ATPases. When the normal protein folding and secretory process are challenged, the accumulation of unfolded or misfolded protein in the lumen occurs and causes ER stress [82, 83]. To restore the homeostasis of ER, a series of responses to stress, called unfolded protein response (UPR) is activated. However, if the damage is impossible to compensate for, ER stress is known to induce cell death [84]. ER stress has been involved in many diseases such as Alzheimer's disease [85], infections and inflammation [86, 87], cardiovascular diseases [88] and cancer [89].

Three different signaling transmembrane receptors of ER have been well-defined by previous studies. They are PKR-like ER kinase (PERK), inositol-requiring enzyme 1 (IRE1) and activating transcription factor 6 (ATF6) [81, 83]. The first two are classified as type I transmembrane proteins while ATF6 is a type II transmembrane protein which exposes N-terminus in the cytosol.

In general, the terminus of these signaling proteins in the ER lumen binds to an ER chaperon, called glucose-regulated protein (GRP) 78 or BiP [82]. As the unfolded proteins begin to accumulate, BiP is released from them to bind to unfolded proteins and thus allows transmembrane receptors to aggregate.

After dissociation of BiP, PERK undergoes oligomerization and autophosphorylation to activate itself. As a eukaryotic initiation factor 2 α (eIF2 α)

kinase, PERK inhibits eIF2 α by phosphorylating it at Ser51 so that translation is repressed globally. This signaling is important to reduce unfolded proteins in the ER. Simultaneously, translation of some mRNAs including a transcription factor ATF4 is activated [90]. Besides facilitating expression of C/EBP homologous protein (CHOP), ATF4 also induces growth arrest and DNA damage-inducible gene 34 (GADD34), which reverses inhibition of translation by eIF2 α dephosphorylation [91, 92].

IRE1 has a similar activation mechanism after dissociation of BiP, though the role of BiP may not be dominant in its activity [93]. In addition to serve as a kinase, it also works as a unique endoribonuclease that cuts away an intron from X box protein-1 (XBP-1) mRNA. This activity contributes to subsequent translation of the protein [94]. XBP-1 is considered to be one part of adaptation mechanism because it upregulates genes that restore normal protein folding and promote protein degradation [95, 96].

For activation of ATF6, it translocates to Golgi apparatus after dissociation from BiP, where it is cleaved by site-1 and site-2 proteases [97]. Cleaved ATF6 is able to migrate into cytosol and then enter nucleus to act as a transcription factor to induce expression of target genes including BiP. Moreover, ATF6 also promotes transcription of XBP-1 mRNA [94].

CHAPTER 2 : EFFECT OF ALPHA 2,6 SIALYLATION ON INTEGRIN-MEDIATED ADHESION OF BREAST CANCER CELLS TO FIBRONECTIN AND COLLAGEN IV

Introduction

The avidity of integrins to their ligands is not only affected by surface expression level, but also regulated by glycosylation. Integrins, glycoproteins composed of α and β subunits, are known receptors of extracellular matrix (ECM) [98]. The interactions between integrins and ECM have been shown to mediate diverse physiological functions such as cell adhesion, development and carcinogenesis [99]. As a basic function carried out by integrins, adhesion to ECM on endothelial and stromal cells is thought to participate in cancer cell metastasis by facilitating extravasation of circulating cancer cells [100]. In addition, integrin mediated adhesion also contributes to the resistance of cancer cells to chemotherapeutic drugs [101] and ionizing radiation [102]. The function of integrins is not only regulated by surface protein expression, but is also controlled by signaling pathways, which confer conformation changes between low and high affinity states [103, 104].

The alteration of integrin sialylation is also an important regulator of cell adhesion, especially sialylation of $\beta 1$ integrin. Mitogen-activated protein kinase/ERK kinase (MEK) activation in U937 myeloid cells induced hyposialylation of $\beta 1$ integrin and increased the avidity of U937 cell adhesion to fibronectin [105]. In contrast, upregulation of ST6Gal-I in metastatic colon cancer

cells led to the elevation of α 2,6 sialylated β 1 integrin, yet also enhanced cell adhesion, migration and metastasis [106, 107]. Ras activation increased α 2,6 sialylation of β 1 integrin of HD3 colonocytes, and desialylation by sialidase inhibited cell adhesion to collagen I [108]. Application of a fluorinated sialic acid analogue has shown great potential in reducing B16F10 melanoma cell adhesion to ECM and tumor growth in mice, which is encouraging for developing drugs targeting hypersialylation in cancer [109]. In light of the importance of α 2,6 sialylation of integrins in the regulation of adhesion of these types of cells, we sought to determine the role of α 2,6 sialylation of integrins in regulating adhesion and invasion of breast cancer cells to ECM. Our data indicate that integrins are highly α 2,6 sialylated on MDA-MB-231 cells but not on MCF-7 cells. Desialylation of integrins increases adhesion of MDA-MB-231 cells to ECM without alteration of integrin expression. Moreover, the desialylation-increased adhesion does not correlate with the migration and invasiveness of the cells.

Materials and Methods

Cell Culture

The breast cancer cell line MDA-MB-231 was kindly provided by Dr. Jianjian Li (University of California Davis Cancer Center, CA), and the breast cancer cell line MCF-7 was obtained from the American Type Culture Collection (Manassas, VA). MDA-MB-231 cells were cultured in minimal essential medium (MEM) (Corning, Manassas, VA), containing 10% fetal bovine serum (Atlanta Biologicals, Lawrenceville, GA), 1 mM sodium pyruvate, 1X non-essential amino

acids (NEAA) and 1% penicillin and streptomycin. MCF-7 cells were cultured in Dulbecco's Modified Eagle Medium (DMEM) supplemented with 10% fetal bovine serum and 1% penicillin and streptomycin.

Antibodies and Reagents

Sialidase from *Vibrio cholerae* [110] (VC, broad substrate specificity) was purchased from Roche (Indianapolis, IN). *Clostridium perfringens* sialidase [111, 112] (CP, specificity of cleavage: α 2,3 > α 2,6 sialylation) and *Arthrobacter ureafaciens* sialidase [113, 114] (AU, specificity of cleavage: α 2,6 > α 2,3 sialylation) were purchased from Sigma-Aldrich (St. Louis, MO) and Prozyme (Hayward, CA), respectively. An ECM screening kit containing fibronectin and collagen IV pre-coated strips was obtained from EMD Millipore (Billerica, MA). The following anti-human primary antibodies were purchased from BD Biosciences (San Jose, CA): CD29 (Mab13) mAb, CD15 (HI98) mAb, CD15s (CSLEX1) mAb, CD49b (12F1) mAb and CD49f (GoH3) mAb. Monoclonal anti-human CD49d (HP2/1) and CD49e (SAM1) were purchased from Beckman Coulter (Indianapolis, IN). The following anti-human primary antibodies were obtained from Santa Cruz Biotechnology (Santa Cruz, CA): CD49e (JBS5) mAb, CD49e (H-104) polyclonal antibody, CD49b (H-293) polyclonal antibody and CD29 (N-20) polyclonal antibody. Anti-activated integrin β 1 antibody (HUTS-4) was purchased from EMD Millipore (Billerica, MA). Biotin conjugated *Sambucus nigra* lectin (SNA) was obtained from EY labs (San Mateo, CA). Corresponding isotype control antibodies, fluorescein isothiocyanate (FITC) conjugated

secondary antibodies, and FITC-conjugated streptavidin were purchased from BD Biosciences. Horse radish peroxidase (HRP) conjugated secondary antibodies were obtained from Santa Cruz Biotechnology. Streptavidin agarose resin was obtained from Thermo Scientific (Rockford, IL).

Western Blotting and Lectin Affinity Assay

For western blotting, MDA-MB-231 and MCF-7 cells were first lysed in 2% NP-40 buffer containing protease inhibitor on ice. Supernatant was collected by centrifugation. Proteins (100 µg) were separated in 8% sodium dodecyl sulfate polyacrylamide gel electrophoresis (SDS-PAGE) resolving gel and transferred to a nitrocellulose membrane (Pall, Port Washington, NY). After blocking for 1 h with 5% non-fat milk in Tris-buffered saline with Tween (TBS-T) at room temperature, the membrane was incubated with anti-CD49b (H293), anti-CD49e (H-104), or anti-CD29 (N-20) antibodies at 4°C overnight. After washing with TBS-T three times, the membrane was incubated with corresponding HRP conjugated secondary antibodies for 30 min at room temperature. Blots were washed with TBS-T and Tris-buffered saline (TBS) twice respectively and visualized using West Pico Supersignal chemiluminescent substrate (Pierce, Rockford, IL). β -actin was used as the loading control.

For the lectin affinity assay, cell lysates (300 µg) of MDA-MB-231 and MCF-7 cells were incubated with 50 µg/ml biotinylated SNA, a specific lectin for α 2,6 sialylation [115, 116], at 4°C overnight. Streptavidin agarose resin (Thermo Scientific, Waltham, MA) was added to cell lysates for 4 h rotation at 4°C. The

beads were then washed once with TBS/1% Triton X-100 and twice with TBS/0.5% Triton X-100. Bead-protein complexes were boiled in SDS-PAGE loading buffer, and released proteins were electrophoresed on an 8% SDS-PAGE as described above. Since β -actin cannot be precipitated by the resin, the loading control (β -actin) for lectin affinity assay was run in a separate gel using the cell lysates before adding biotinylated SNA.

Flow Cytometry

Surface sialylation and integrin expression were assessed by flow cytometry. MDA-MB-231 and MCF-7 cells were collected in phosphate buffered saline (PBS) and washed twice. Cells were then fixed in 4% formaldehyde for 10 min. After being chilled on ice for 60 s, cells were washed once in PBS, and twice in 0.5% bovine serum albumin (BSA) before resuspension in 0.5% BSA for blocking. 1×10^6 cells were incubated with primary mAb anti-CD15s (CSLEX1), anti-CD15 (HI98), anti-CD49b (12F1), anti-CD49e (JBS5), anti-CD29 (Mab13), anti-CD29 (HUTS-4), biotinylated SNA and corresponding isotype control antibodies for 1 h at room temperature. For biotinylated SNA, the FITC-conjugated streptavidin was used as background control. For CD15 and CD15s, the secondary antibody alone was used as background. After washing with 0.5% BSA twice, cells were incubated with corresponding FITC conjugated secondary antibodies for 30 min at room temperature. Cells were washed twice with 0.5% BSA, resuspended in 0.5 ml PBS and analyzed on a FACSAria Special Order Research Product flow cytometer (BD Biosciences).

Cell Adhesion Assay

Adhesion of MDA-MB-231, MCF-7 and HT-29 cells to fibronectin was measured using ECM coated strips (EMD Millipore) per the manufacturer's instructions. Briefly, cells were collected, washed and resuspended in culture medium. 2×10^5 MDA-MB-231 cells, 3×10^5 MCF-7 cells and 1×10^5 HT-29 cells were seeded onto fibronectin coated strips. Cells were incubated for 30 min at 37°C. Strips were washed by DPBS to remove non-adherent cells. 0.2% Crystal violet in 10% ethanol was used to stain attached cells and the cells were finally dissolved in 2% SDS after washing. Absorbance at 540 nm was measured by a microplate reader (Molecular Devices, Sunnyvale, CA). Absorbance was normalized to the control cells incubated in DPBS without sialidase.

Cell Migration and Invasion Assay

For migration, a wound-healing assay was performed as previously described with modifications [117]. A 96-well plate for suspension culture (Greiner Bio-One, Monroe, NC) was coated with $2 \mu\text{g}/\text{cm}^2$ fibronectin overnight at 4°C. Then the cells were mock treated or treated with sialidases, and monolayer wounds were created using a 200 μL pipette tip. The cells were washed once with serum free medium and allowed to migrate for 7 h in FBS free DMEM. The wound healing was visualized using an Olympus IX70 inverted microscope (Olympus, Tokyo, Japan) at 4X magnification. Photographs were taken by a Retiga 1300 CCD Camera (Qimaging, Burnaby, B.C., Canada) using iVision-Mac™ software (BioVision Technologies, Exton, PA). The width of the wound

(gap distance) was measured by ImageJ (National Institutes of Health, Bethesda, MD). Gap distances were shown as the ratio of 7 h to 0 h.

For the invasion assay, 8 μm pore Polycarbonate Membrane Transwell® Inserts in 24-well plates (Corning, Tewksbury, MA) were used per the manufacturer's instructions. Inner chambers of transwell inserts were first coated with 20 $\mu\text{g/ml}$ fibronectin overnight at 4°C. Cells were mock treated or treated with sialidases. After washing once with serum free medium, the cells (1×10^5) were suspended in 100 μL FBS free medium and seeded onto each inner chamber. 600 μL DMEM with 10% FBS was added to the outer chambers. Transwell inserts were incubated for 24 h at 37°C. Cells that migrated into the lower surface of the membrane were fixed by 4% formaldehyde and stained with crystal violet. In each experiment, cells were counted in 4 different fields. Cells were imaged by the same digital camera and software as described above.

Statistical Analysis.

The data are presented as mean \pm SD of at least 3 independent experiments. Student's *t*-test was used in comparing control group and each treatment. Only $p < 0.05$ was considered statistically significant.

Results

$\alpha 5\beta 1$ and $\alpha 2\beta 1$ integrins on MDA-MB-231 but not MCF-7 cells are $\alpha 2,6$ sialylated

To determine the role of sialylation of integrin in breast cancer cell adhesion, we first determined the expression and sialylation on $\alpha 5\beta 1$ and $\alpha 2\beta 1$ integrin. They play critical roles in regulation of adhesion of breast cancer MDA-

MDA-MB-231 or MCF-7 cells to ECM proteins, specifically collagen IV (Col IV) and fibronectin. The contribution of $\alpha 5\beta 1$ and $\alpha 2\beta 1$ in adhesion of MDA-MB-231 or MCF-7 cells was confirmed using a monoclonal antibody blockade assay (Fig 2.1). Our data indicate that $\alpha 2$, $\alpha 5$ and $\beta 1$ integrins were expressed in both cell lines, and MDA-MB-231 expressed a higher level of each integrin compared to MCF-7 cells (Fig 2.2, right panel). In view of the importance of $\alpha 2,6$ sialylation in regulating cell adhesion, lectin SNA was used as an $\alpha 2,6$ sialylation marker to compare the sialylation level between the two breast cancer cell lines. However, only the integrins on MDA-MB-231 were heavily $\alpha 2,6$ sialylated; the $\alpha 2,6$ sialylation of integrins on MCF-7 cells was nearly undetectable by lectin affinity assay (Fig 2.2, left panel).

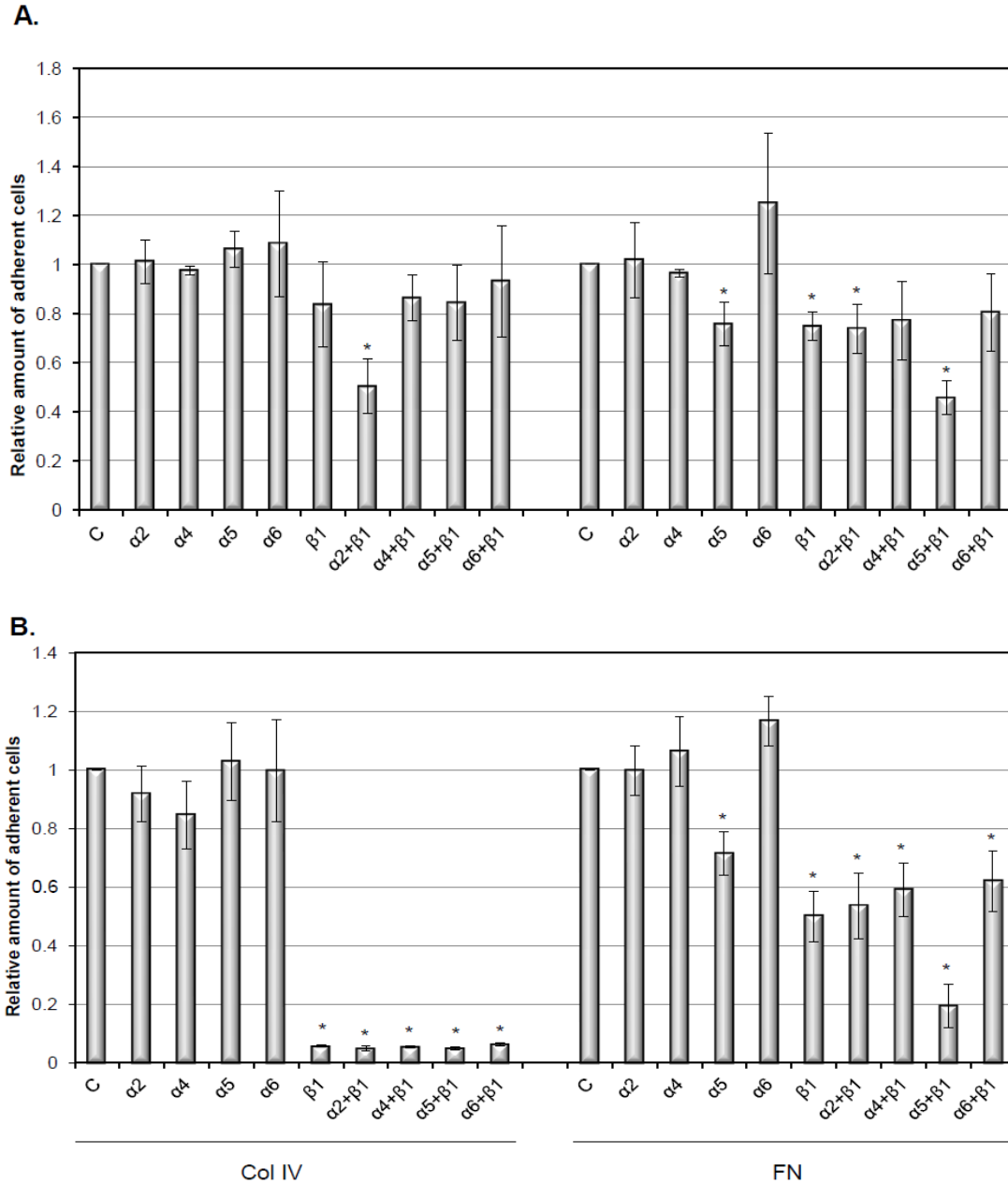


Figure 2.1 Monoclonal antibody blockade assay. MDA-MB-231(A) and MCF-7 (B) cells were treated with 20 $\mu\text{g}/\text{ml}$ monoclonal antibody against $\alpha 2$, $\alpha 4$, $\alpha 5$, $\alpha 6$ and $\beta 1$ integrin for 1h at room temperature. Antibodies against $\beta 1$ and α integrins were added together to block $\alpha 2\beta 1$, $\alpha 4\beta 1$, $\alpha 5\beta 1$ and $\alpha 6\beta 1$ integrins. 1.5×10^5 MDA-MB-231 and MCF-7 cells were seeded into each well of fibronectin (FN) and collagen IV (Col IV) pre-coated strips. Cells were washed and stained after 30 min incubation at 37°C . Duplicate samples were prepared in each experiment. Data shown are the means \pm SD, $n=3$ independent experiments. *: $p < 0.05$ versus untreated control group.

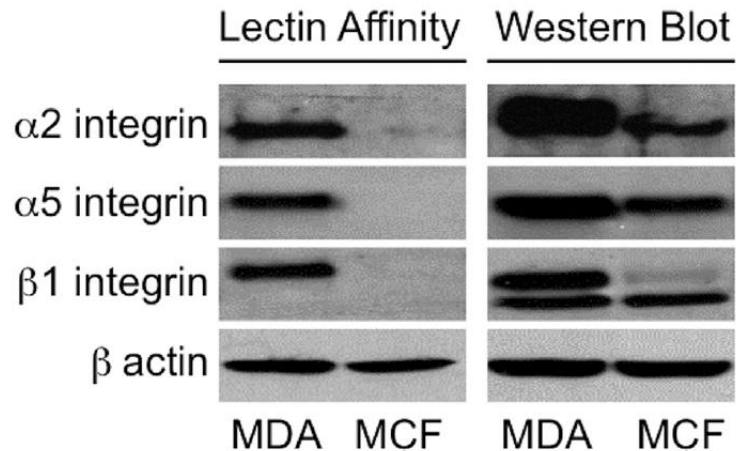
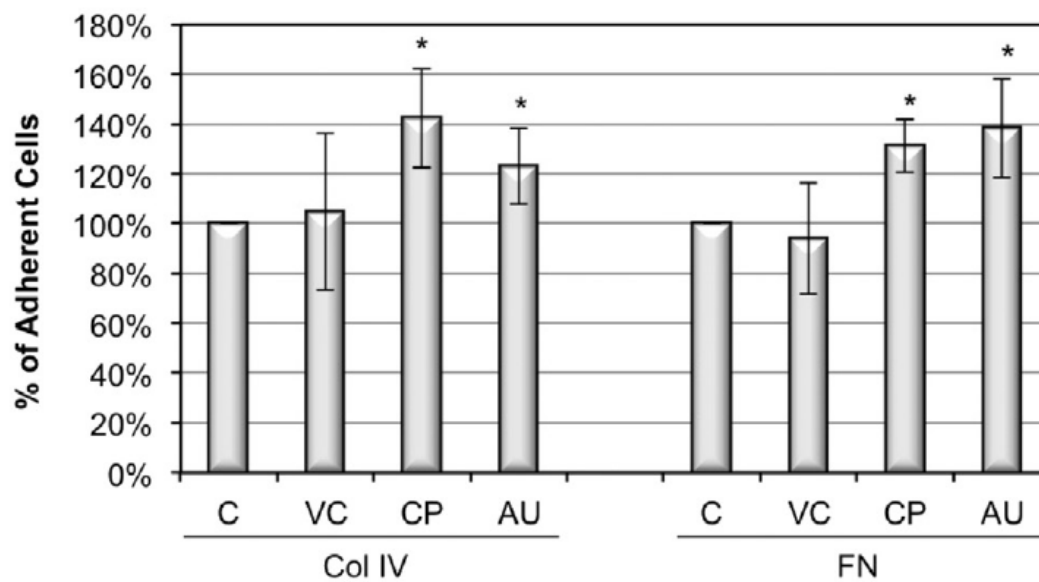
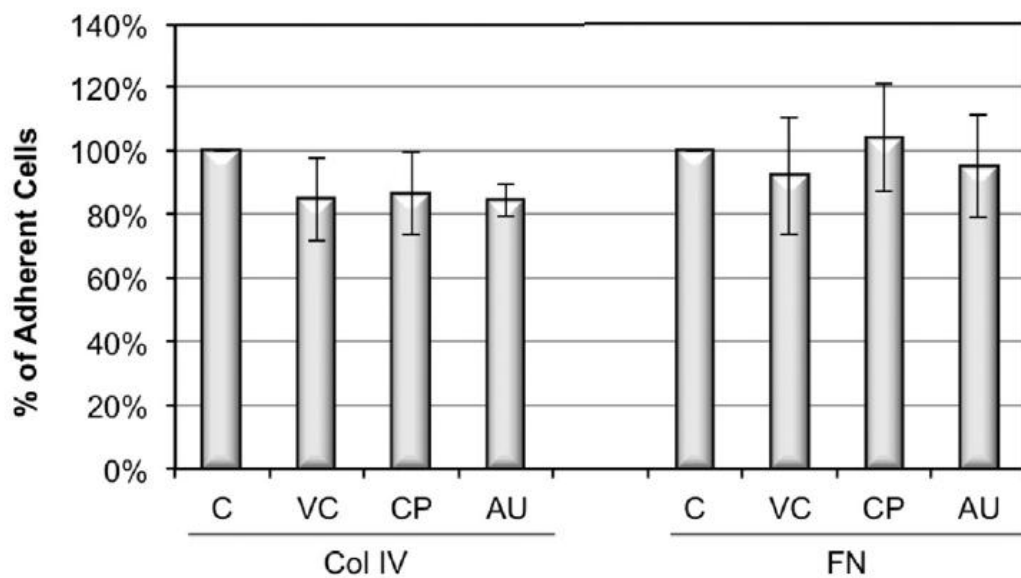


Figure 2.2 Sialylation of relevant integrins on MDA-MB-231 and MCF-7 cells. For lectin affinity assay, 300 μ g cell lysate of MDA-MB-231 and MCF-7 cells were harvested and incubated with 50 μ g/ml biotinylated SNA at 4°C overnight. Streptavidin agarose beads were then added for additional 4 hours incubation at 4°C. Beads were washed and boiled before loading to the gel. Loading control for lectin affinity assay was collected before adding biotinylated SNA. For western blotting, 100 μ g cell lysate was loaded. This figure is representative of 3 independent experiments.

Desialylation of $\alpha 2,6$ -sialylated integrins increases adhesive affinity between MDA-MB-231 cells and ECM proteins

To determine the involvement of $\alpha 2,6$ sialylation in mediating breast cancer cell adhesion, we tested the effect of three sialidases with different specificities on adhesive affinities between $\alpha 2\beta 1$ integrin and Col IV, and between $\alpha 5\beta 1$ and fibronectin. *V. cholera* (VC) sialidase has broad cleavage activity (i.e., no specificity preference for sialic acid linkages) [110]; and *C. perfringens* (CP) and *A. ureafaciens* (AU) sialidases have a preference towards $\alpha 2,3$ sialylation [111, 112] and $\alpha 2,6$ sialylation [113, 114], respectively. Our data showed that the attachment of MDA-MB-231 cells to collagen IV was increased

to $142.2\% \pm 19.9\%$ or $123.1\% \pm 15.4\%$ after CP sialidase or AU sialidase treatment, respectively (Fig 2.3A). The attachment of MDA-MB-231 cells to fibronectin was increased to $131.3\% \pm 10.7\%$ and $138.1\% \pm 19.7\%$ after CP sialidase and AU sialidases treatment, respectively (Fig 2.3A). As expected, under the same conditions, the attachment of MCF-7 cells to collagen IV or fibronectin did not increase (Fig 2.3B). However, it was a surprise that VC sialidase had no statistically significant effect on breast cancer cell adhesion, given its ability to cleave sialic acids of multiple linkages (Fig 2.3A). Further analysis using a sialylated integrins-expressing colon cancer cell line HT-29 [118] demonstrated that the same VC sialidase treatment decreased adhesion to collagen IV by $70\% \pm 1.9\%$ (Fig 2.3C), which is in agreement with a previous report [119]. Interestingly CP and AU sialidases had no statistically significant effects on HT-29 cell adhesion (Fig 2.3C), suggesting the specificity of sialidases might be cell line dependent.

A. MDA-MB-231 Cells**B. MCF-7 Cells**

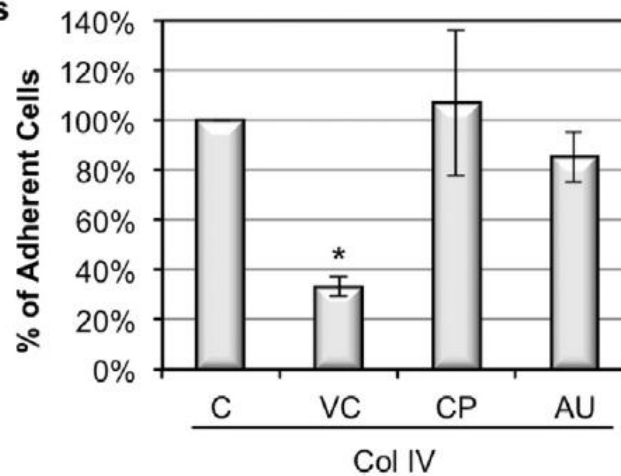
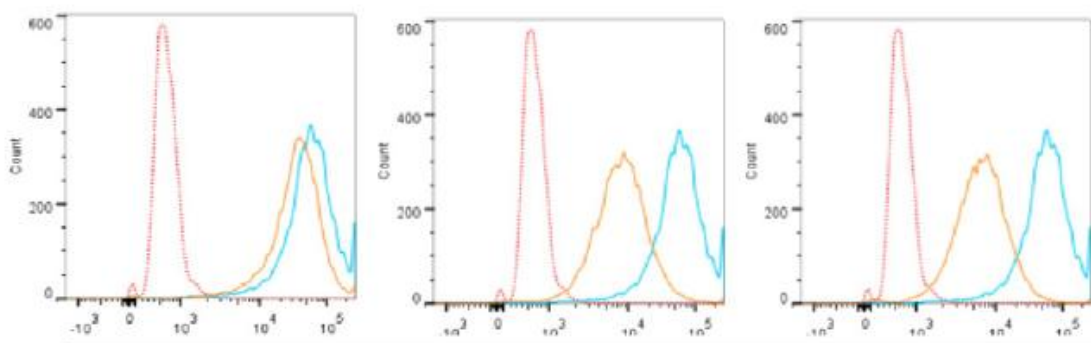
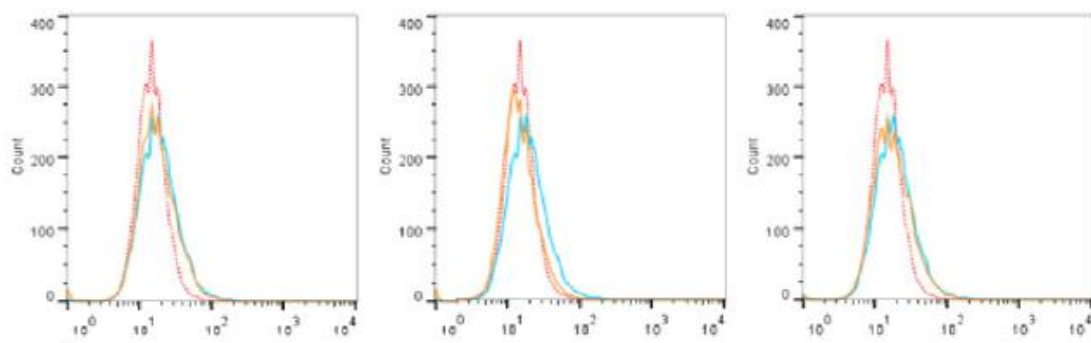
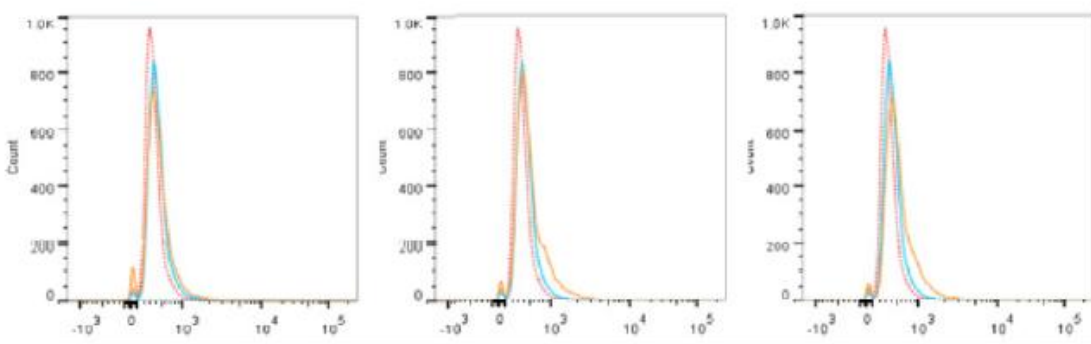
C. HT-29 Cells

Figure 2.3 Effect of sialidase on adhesion of MDA-MB-231 cells, MCF-7 cells and HT-29 cells to ECM.

(A) MDA-MB-231 cells, (B) MCF-7 cells and (C) HT-29 cells were harvested and treated with 0.1U/ml *V. cholera* (VC), *C. perfringens* (CP), and *A. ureafaciens* (AU) sialidase in DPBS for 30 min at 37°C. Cells were seeded into each well of fibronectin (FN) or collagen IV (Col IV) pre-coated strips. Cells were washed and stained after 30 min incubation at 37°C. Absorbance was normalized to the control cells incubated in DPBS without sialidase. Duplicate samples were prepared in each experiment. Data shown are the means \pm SD, n=5. *: $p < 0.05$ versus untreated control group.

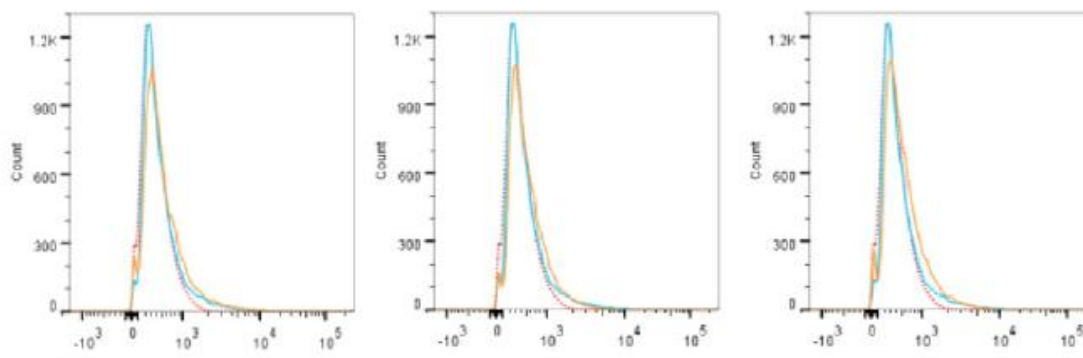
Since VC sialidase, which should cleave both $\alpha 2,6$ and $\alpha 2,3$ linked sialic acids, did not have a significant effect on the cell adhesion, we examined specificities of the sialidases using lectin SNA as $\alpha 2,6$ sialylation marker and CD15s/CD15 ratio as $\alpha 2,3$ sialylation markers, in removing sialic acids. Our data showed that lectin SNA-binding on MDA-MB-231 cells was reduced by 5.8% \pm 1.3%, 58.5% \pm 14.5% and 84.3% \pm 0.5% after treating with VC, CP and AU sialidase respectively (Fig 2.4A, C). This result confirmed that CP and AU sialidases are more efficient in cleaving $\alpha 2,6$ sialylation than VC sialidase. Our data also showed that endogenous CD15S expression on MDA-MB-231 cells

was very weak and none of the sialidase treatments had any effect on CD15S/CD15 ratio on the cells (Fig 2.4A, C). As for MCF-7 cells, the lectin SNA-binding and CD15S expression were hardly detected. Thus the sialidase treatment did not have any effect on these markers as expected (Fig 2.4B, D).

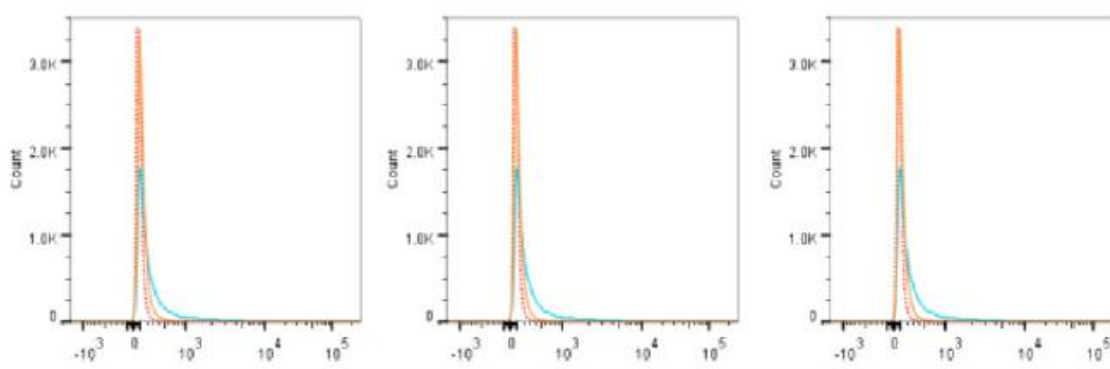
A. MDA-MB-231*V. cholerae**C. perfringens**A. ureafaciens***SNA-FITC****CD15S-FITC****CD15-FITC**

B. MCF-7

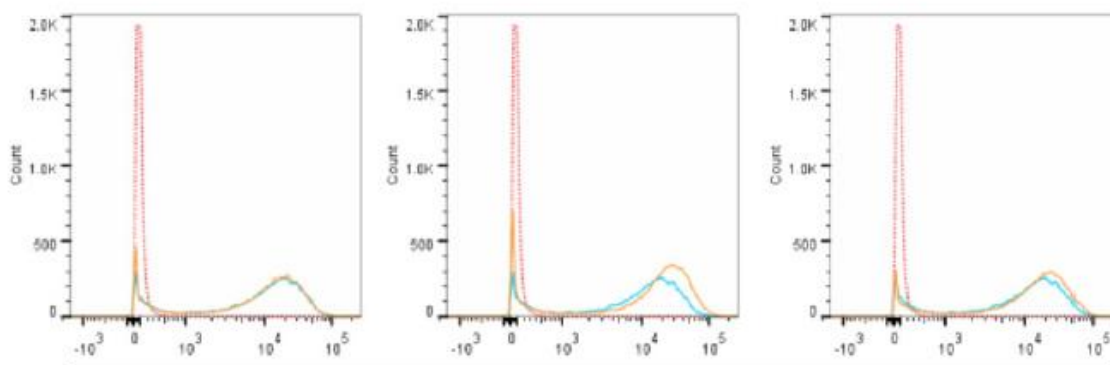
V. cholerae *C. perfringens* *A. ureafaciens*



SNA-FITC

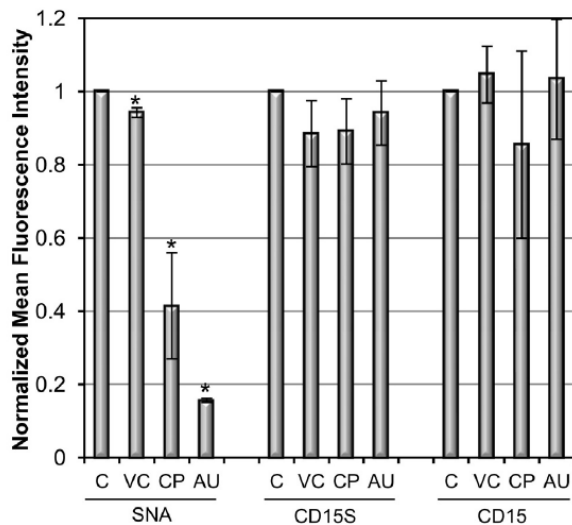


CD15S-FITC



CD15-FITC

C. MDA-MB-231



D. MCF-7

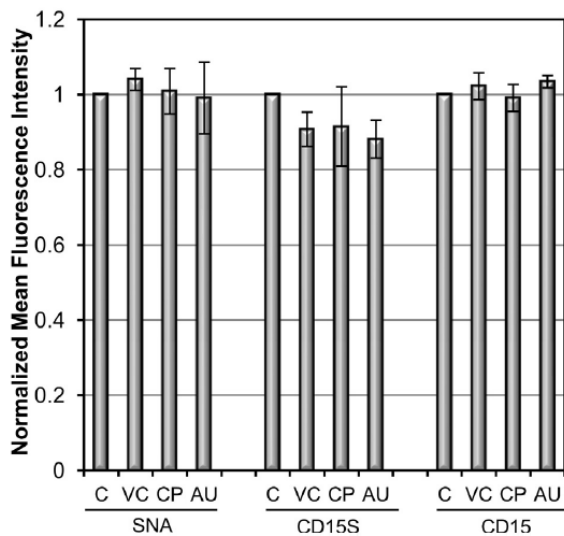
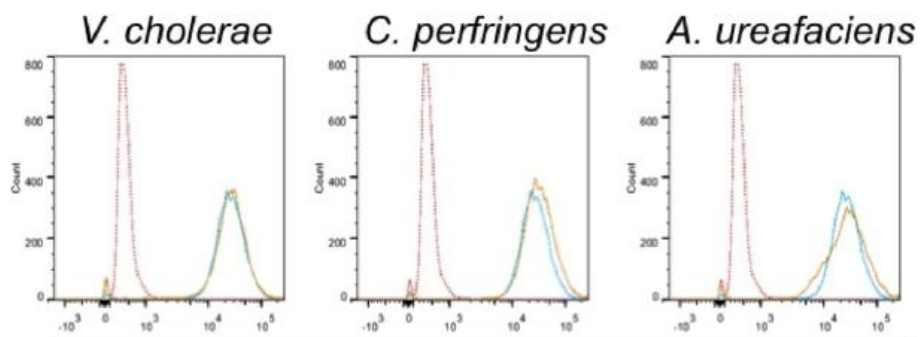
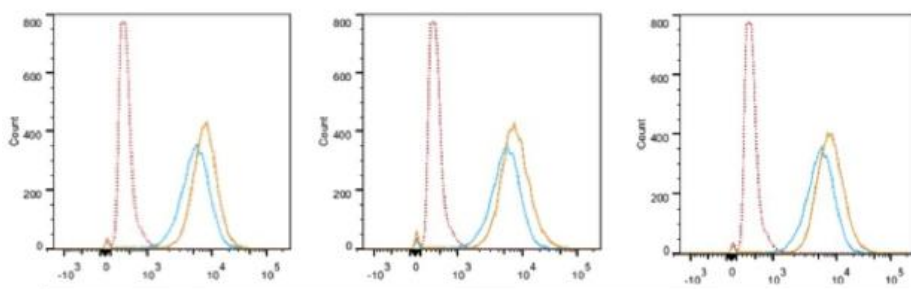
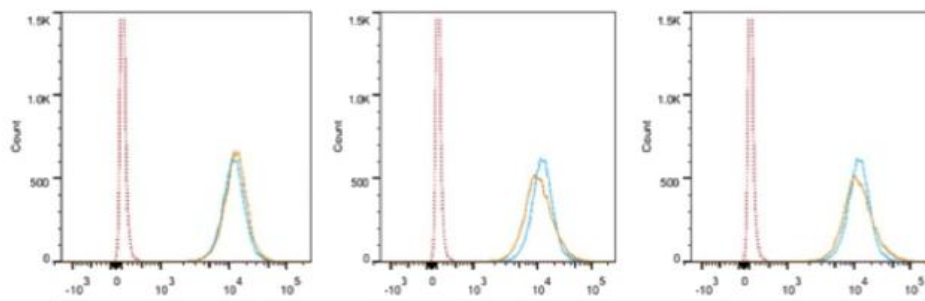
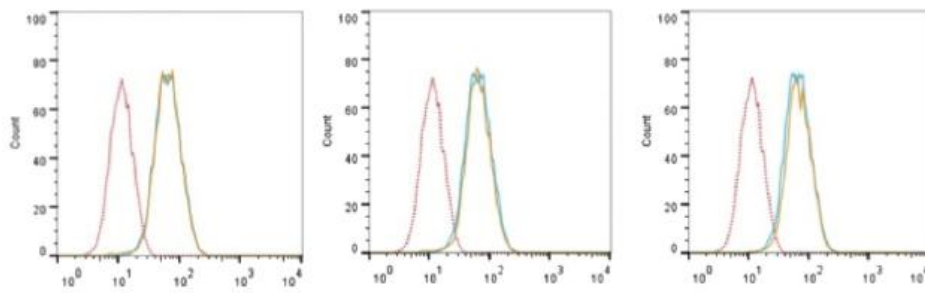


Figure 2.4 Detection of sialic acid cleavage on MDA-MB-231 and MCF-7 cells by flow cytometry after sialidase treatment.

(A) MDA-MB-231 and (B) MCF-7 cells were harvested and treated with 0.1U/ml *V. cholera* (VC), *C. perfringens* (CP), or *A. ureafaciens* (AU) sialidase in DPBS for 30 min at 37°C. SNA binding, CD15 expression and CD15s expression on MDA-MB-231 and MCF-7 cells were measured by flow cytometric analysis. Red dotted lines represent background (secondary antibody alone), blue lines represent control cells incubated in DPBS without sialidase and orange lines represent sialidase treated cells. Quantification of flow cytometry by normalizing mean fluorescence intensity relative to control cells is shown in C and D. These figures are representative of 3 independent experiments.

To eliminate the possibility that the changes in adhesion to Col IV and fibronectin were due to the surface integrin expression level changes after sialidase treatment, flow cytometry was used to analyze cells. In MDA-MB-231 cells, there was no significant change in any integrins (Fig 2.5A). In MCF-7 cells, β 1 integrin level did not change after sialidase treatment (Fig 2.5B). In addition, activated β 1 integrin was also tested under the same conditions, and no significant change was observed in either cell line (Fig 2.5). These data indicate that the increased adhesion resultant with sialidase treatments is not due to a change in surface expression or activation of β 1 integrin.

A. MDA-MB-231**Alpha 2-FITC****Alpha 5-FITC****Beta 1-FITC****Activated beta-1-FITC**

B. MCF-7

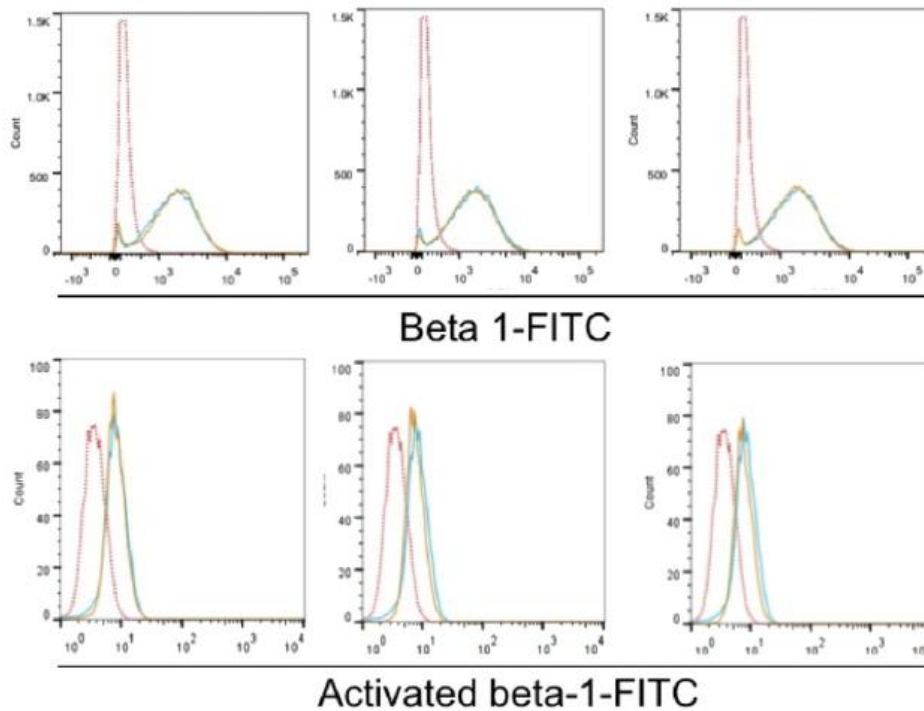


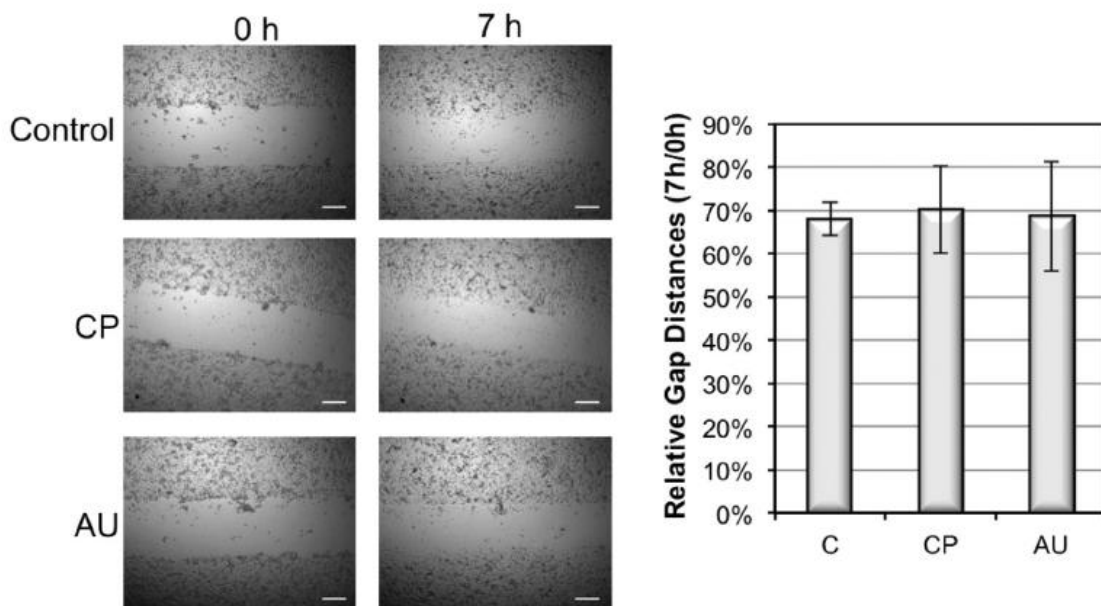
Figure 2.5 Surface expression of relevant integrins on MDA-MB-231 and MCF-7 cells after sialidase treatment.

(A) MDA-MB-231 cells and (B) MCF-7 cells were harvested and treated with 0.1U/ml *V. cholerae*, *C. perfringens*, and *A. ureafaciens* sialidase in DPBS for 30 min at 37°C. Expression of $\alpha 5$, $\beta 1$ and activated $\beta 1$ integrin on MDA-MB-231 cells, and $\beta 1$ integrin and activated $\beta 1$ integrin on MCF-7 cells were analyzed by flow cytometry. Red dotted lines represent isotype control, blue lines represent control cells incubated in DPBS without sialidase treatment and orange lines represent sialidase treated cells. These figures are representative of 3 independent experiments.

Sialidase-catalyzed integrin desialylation does not correlate with MDA-MB-231 cell migration and invasion

To determine whether the desialylation and increased adhesion of MDA-MB-231 cells are correlated to the later metastatic cascade steps of migration and invasion, we examined migration and invasion of desialylated cells on fibronectin-coated surface using wound healing assay and transwell invasion assay. Our data indicate that CP or AU sialidase treatments have no statistically significant effects on migration and invasiveness of the cells (Fig 2.6). As CP and AU were confirmed to be the most efficient sialidases cleaving $\alpha 2,6$ sialylation on MDA-MB-231 cells, these data together indicate that decreasing $\alpha 2,6$ sialylation by sialidase treatment does not affect cell migration and invasion, regardless of the influence on cell adhesion.

A.



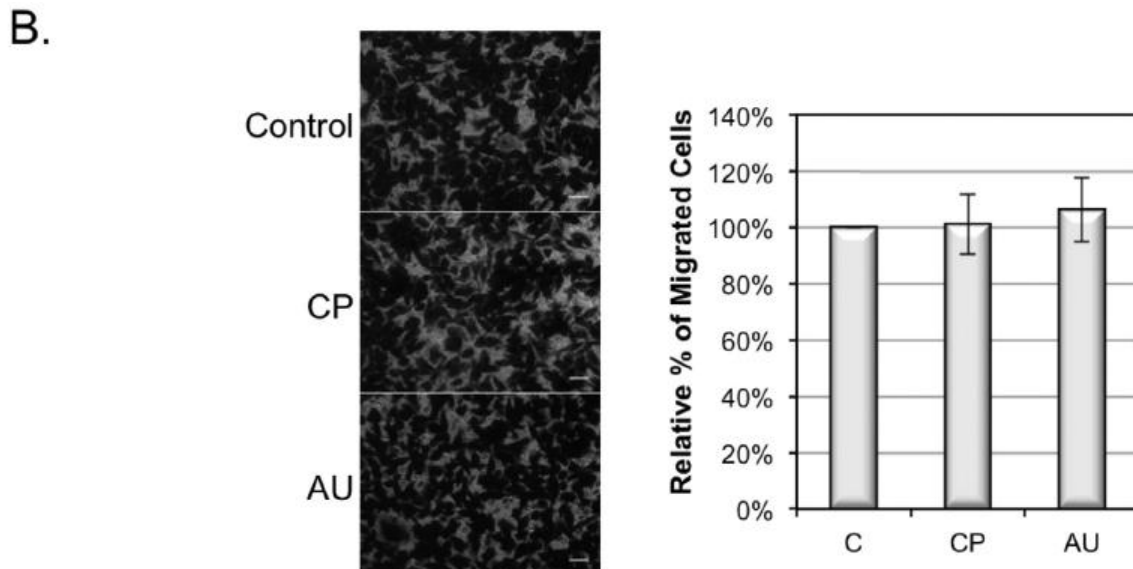


Figure 2.6 Effect of sialidase on migration and invasion of MDA-MB-231 cells. (A) MDA-MB-231 cells were grown on a fibronectin-coated plate to reach confluence and were treated with 0.1U/ml *C. perfringens* (CP), and *A. ureafaciens* (AU) sialidase in DPBS for 30 min at 37°C. The wound was then made using a 200 μ l pipette tip. Cells were incubated in FBS free medium for 7 h at 37°C. Photographs were taken at 0 h and 7 h. Gap distances were shown as the ratio of 7 h to 0 h. Duplicate samples were prepared in each experiment. Data shown are the means \pm SD, n=4. *: p<0.05 versus control group. Scale bar, 250 μ m. (B) MDA-MB-231 cells were harvested and treated with sialidases as described in (A). 1×10^5 MDA-MB-231 cells were seeded into inner chamber of transwell inserts coated with fibronectin (FN). After 24 h incubation at 37°C, cells migrated to the lower surface were fixed, stained and then counted under a microscope from 4 different fields. Duplicate samples were prepared in each experiment. Data shown are the means \pm SD, n=3. *: p<0.05 versus control group. Scale bar, 50 μ m.

Discussion

Altered glycosylation of integrins plays roles in cancer cell adhesion, migration and invasion during metastasis [120-124]. As one of a diverse family of sialylated integrins, α 2,6 sialylated β 1 integrin has been identified in many types of cancer cells, such as ovarian cancer cells (SKOV3 and PA1) [122], colon cancer cells (SW480, Lovo) [124], and melanoma cells (WM9 and WM239)

[125]. However, the role of sialylation on breast cancer cells in regulation of cell adhesion is not fully understood. It has been reported that antisense transfection of ST6 Gal-I decreased adhesion of MDA-MB-435 breast cancer cells to collagen IV [126]. But MDA-MB-435 cells were later found to originate from M14 melanoma cells [127], leaving a need to investigate the differential sialylation of integrins on widely used breast cancer cells, for instance MDA-MB-231 and MCF-7 cells, and the role(s) in cell adhesion. In this study, we determined the regulatory roles of sialylation on $\alpha 5\beta 1$ and $\alpha 2\beta 1$ integrins, which mediate the adhesion of breast cancer cells to ECM proteins [128]. We demonstrated that MDA-MB-231, but not MCF-7, cells are highly sialylated with $\alpha 2,6$ linked sialic acids on $\alpha 2$, $\alpha 5$ and $\beta 1$ subunits of the integrins (Figs 2.2 and 2.5); and that $\alpha 2,6$ sialylation reduces the affinity between MDA-MB-231 cells to collagen IV and fibronectin (Fig 2.3). These results agree with previous findings with leukemic cells [105, 129, 130]. Nevertheless, the results contrast with large amount of reports based on the studies of colon cancer cells indicating $\alpha 2,6$ sialylation on $\beta 1$ integrin promotes the cell adhesion to ECM proteins laminin and collagens [106, 107, 119]. Thus, our results further confirm that the regulation of integrin function by sialylation is not uniform across different cancer cell types. Moreover, our results also demonstrate that the sialylation-increased adhesion of MDA-MB-231 cells is not correlated with migration and invasiveness of the cells (Fig 2.6). These results, together with previous reports [131-134], strongly indicate that

sialylated integrin-mediated cancer adhesion does not have a direct correlation with cancer cell migration and invasiveness.

CHAPTER 3 : THE ROLE OF ROS IN IONIZING RADIATION-INDUCED VLA-4 MEDIATED ADHESION OF RAW264.7 CELLS TO VCAM-1 UNDER FLOW CONDITIONS

Introduction

Radiation therapy in combination with surgery is a powerful weapon against cancer. Unfortunately, some negative side effects following radiation therapy have been documented. Radiation therapy has been linked closely to cardiovascular diseases, including pericarditis [135], cardiomyopathy [136], valvular disease [137], thrombosis, and arteriosclerosis [72, 73]. Research has demonstrated that chest radiation is a major risk factor of cardiovascular disease: typical examples include radiation effects on hodgkin lymphoma [138, 139] and breast cancer [140]. Additionally, left-sided radiation therapy in breast cancer leads to a higher cardiovascular risk [141]. Despite conflicting data, the comparison between older and newer radiation techniques show the benefit of reducing radiation dose to the chest [142].

Atherosclerosis has been shown to be an inflammatory disease involving monocytes and macrophages [143]. Low-density lipoprotein accumulates on the endothelium and acts as the initiator of atherosclerosis after being oxidized. Oxidized low-density lipoprotein (OxLDL) induces the expression of vascular cell adhesion molecule-1 (VCAM-1) and intercellular adhesion molecule-1 (ICAM-1) on different endothelial cells [144]. Integrins, the heterodimeric receptors composed of different α and β subunits [98] play major roles in the development

of atherosclerosis [145]. Inflammatory monocytes' adhesion involves very late antigen-4 (VLA-4, $\alpha 4\beta 1$ integrins) and $\beta 2$ integrins, although there are conflicting reports as to which molecule plays a more significant role during inflammation [146-149]. After infiltration, monocytes can differentiate into macrophages and appear to be involved in development of atherogenesis. Macrophage homing to the plaque is also responsible for degradation and rupture [150]. E-selectin, ICAM-1 and $\alpha 4\beta 1$ integrins play important roles in macrophage homing [151]. It has been shown that in IL-4 induced leukocytes recruitment, $\alpha 4$ integrins dominate the adhesion when endothelial selectins were blocked [152]. Blocking of VLA-4 effectively reduced the cell adhesion and therefore reduced plaque formation [153, 154].

Over the last two decades, extensive studies have confirmed that endothelium is damaged by ionizing radiation (IR) and that it facilitates leukocytes, lymphocytes and platelet adhesion by up-regulation of ICAM-1, E-selectin, von Willebrand factor (vWF) and platelet endothelial cell adhesion molecule-1 (PECAM-1) [155-158]. However, not enough attention has been given to how IR affects integrins in monocytes/macrophages, since during radiotherapy, not only the vessels, but also the blood cells are irradiated. In light of the importance of VLA-4 in the monocytes/macrophages adhesion, we investigated the role of VLA-4-mediated adhesion under flow conditions, our studies complement the current investigations that focus on the role of endothelial cells in radiation-associated atherosclerosis.

Materials and Methods

Cell Culture

RAW264.7 mouse monocytes/macrophages obtained from the American Type Culture Collection (Manassas, VA) were cultured in Dulbecco's modification of eagle's medium (DMEM) (Corning, Manassas, VA), containing 10% fetal bovine serum (Denville, Metuchen, NJ) and 1% penicillin and streptomycin (Invitrogen, Carlsbad, CA) at 37 °C with 5% CO₂.

Flow Cytometry

Surface expression of integrins on RAW264.7 cells was evaluated by flow cytometer. The cells were pelleted by centrifugation, resuspended in phosphate-buffered saline (PBS) and fixed in 4% formaldehyde for 10 min. 1x10⁶ cells from each sample were rinsed, blocked with 5% bovine serum albumin (BSA) and incubated with FITC-conjugated anti- α 4 integrin (CD49d, 560840, BD Biosciences, Franklin Lakes, NJ) or FITC-conjugated anti- β 1 integrin (CD29, sc-9970 FITC, Santa Cruz Biotechnology, Santa Cruz, CA) for 30 min in the dark. After washing with 5% BSA twice, cells were suspended in 0.5 ml PBS and analyzed on FACSort flow cytometer (BD Biosciences).

Western Blotting

RAW264.7 cells were lysed in 2% NP-40 buffer (2% NP-40, 80 mM NaCl, 0.1% SDS) containing protease inhibitor cocktail set III (Millipore, Darmstadt, Germany). After 15 min incubation on ice the lysates were centrifuged and the supernatants were collected. The proteins (100 μ g) were electrophoresed on an

8% SDS-PAGE, transferred to a nitrocellulose membrane and blocked with 5% non-fat milk in tris-buffered saline with Tween (TBS-T) (USB, Cleveland, OH) for 1 h. Blots were incubated with anti-human $\alpha 4$ integrin (sc-14008, Santa Cruz Biotechnology, Santa Cruz, CA) or anti-human $\beta 1$ integrin (sc-9970, Santa Cruz Biotechnology, Santa Cruz, CA) at 4°C overnight. Membranes were washed with TBS-T three times and probed with corresponding secondary antibodies for 0.5 h at room temperature. Then blots were washed with TBS-T three times and with tris-buffered saline (TBS) twice. The signals were detected using West Pico Supersignal chemiluminescent substrate (Pierce, Rockford, IL).

Parallel Plate Flow Chamber Adhesion Assays

Dynamic flow adhesion assays were performed as previously described [159]. Briefly, cell culture dishes were coated with 25 $\mu\text{g}/\text{mL}$ VCAM-1 (R&D System, Minneapolis, MN) at 4°C overnight. Coated dishes were blocked with 0.1% BSA in Dulbecco's phosphate-buffered saline (DPBS) (Invitrogen, Carlsbad, CA) for 2 h at room temperature and then were washed with DPBS. RAW264.7 cells ($1 \times 10^6/\text{mL}$) in DPBS were perfused through the chamber for 5 min at a shear stress of 1.2 dynes/cm^2 . Cell motility was observed in a 4X field and recorded using Qimaging retiga 1300 videomicroscopy (Qimaging, BC, Canada). The numbers of adherent cells were counted in video.

Statistical Analysis

Student's *t*-test was performed to compare data in the different treatment groups. Data was considered statistically significant when $p < 0.05$.

Results

IR increases surface expression of $\alpha 4$ and $\beta 1$ integrins in RAW264.7 cells.

Since VLA-4 ($\alpha 4\beta 1$ integrins) plays a major role in adhesion between monocytes/macrophages and endothelial cells [151, 153], we first determined the extent of effect of IR on the cell surface expression of $\alpha 4$ and $\beta 1$ integrins. Flow cytometry analysis revealed that both $\alpha 4$ and $\beta 1$ integrins were increased on the cell surface after IR (5 Gy) (Fig 3.1A, B). Despite the fact that there was only slight difference at 8 h, both $\alpha 4$ and $\beta 1$ integrin peaked within 24 h post-IR. Prolonged incubation time did not further increase the surface expression level of the proteins (Fig 3.1A, B). Western blot analysis indicated that, while the expression of total $\alpha 4$ integrin was significantly increased, total $\beta 1$ integrin was not changed at 24 h postirradiation (Fig 3.1C). These results suggest that the increased surface expression of an integrin is not always dependent on an induced expression of that specific integrin after irradiation.

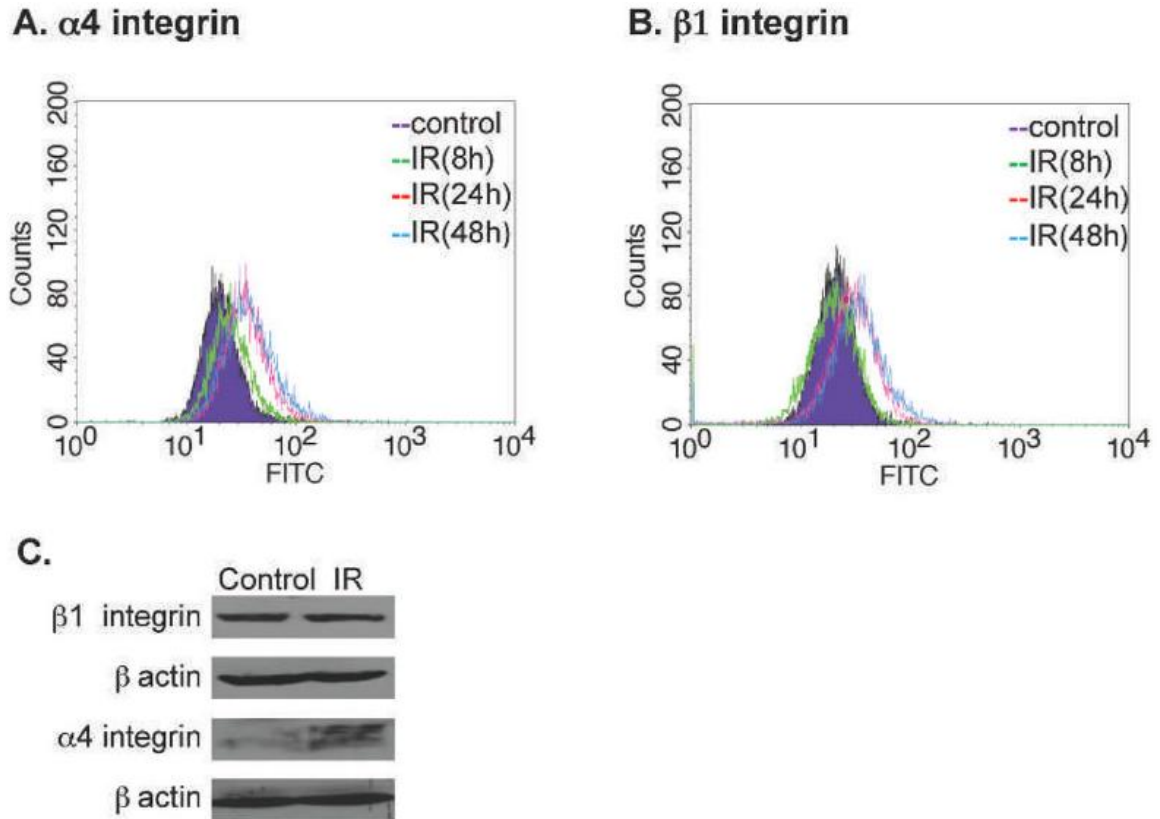


Figure 3.1 Expression of $\alpha 4$ and $\beta 1$ integrins in RAW264.7 cells after ionizing radiation.

RAW264.7 cells were processed for flow cytometry at 8, 24, and 48 hours following 5 Gy irradiation. (A) Surface expression of $\alpha 4$ integrin. (B) Surface expression of $\beta 1$ integrin. (C) Western analysis of $\alpha 4$ and $\beta 1$ integrin. The whole RAW264.7 cell lysate was prepared at 24 h post-irradiation.

IR-altered avidity of RAW264.7 cells to VCAM-1 is not correlated to the surface expression of VLA-4 integrins.

The extent of the effect of IR-induced surface expression of VLA-4 on macrophage adhesion to VCAM-1, the receptor of VLA-4, was assessed using a parallel plate flow chamber assay. Physiological shear stress from 1 to 2 dynes/cm² was examined [160] and a shear stress of 1.2 dynes/cm² was adopted, under these condition there was a stable and countable amount of adhesion cells

in each field of view. Our data indicated that the number of adherent cells to VCAM-1 was reduced by $19.7 \pm 2.7\%$ and $28.4 \pm 4.0\%$ at 8 h and 24 h, respectively, after 5 Gy of ionizing radiation (Fig 3.2A), and is not correlated to the increased VLA-4 expression after the same dose of radiation (Fig 3.2A, B). Our data also revealed that while the affinity between RAW264.7 cells and VCAM-1 was decreased in a dose-dependent manner from 1-5 Gy at 24 h postirradiation, the affinity between the cells and VCAM-1 was increased by $17.3 \pm 4.5\%$ after being treated with 0.5 Gy at 24 h postirradiation (Fig 3.2B).

To determine whether the reduced avidity of the macrophage after higher doses of IR treatment was due to the loss of viability of the cells, we analyzed the percentage of cell death after irradiation. Our data showed that the percentage of dead cells was only increased 11% after 5 Gy of IR and had no statistically significant change after lower doses (0.5 Gy and 1 Gy) of IR (Fig 3.2C). These results indicated that clinical doses of radiation do not result in remarkable cell death at 24 h postirradiation (Fig 3.2C), which agreed with a previous report indicating that macrophages are very resistant to IR [161]. These results also suggest that the altered avidity of macrophage to VCAM-1 is not correlated to the IR-induced surface expression of VLA-4 and cell death.

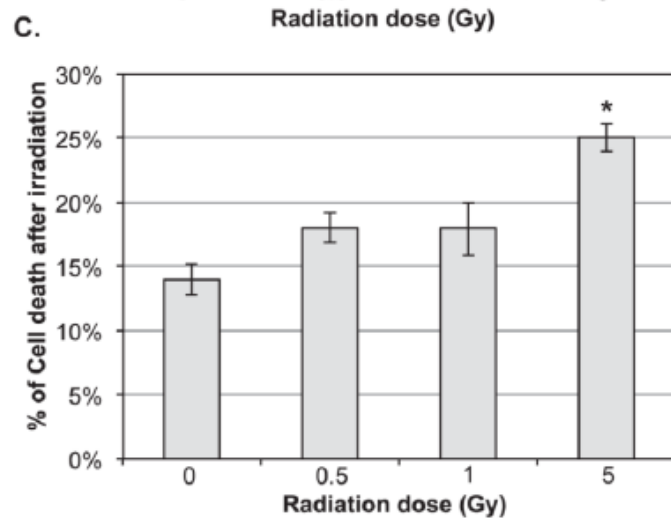
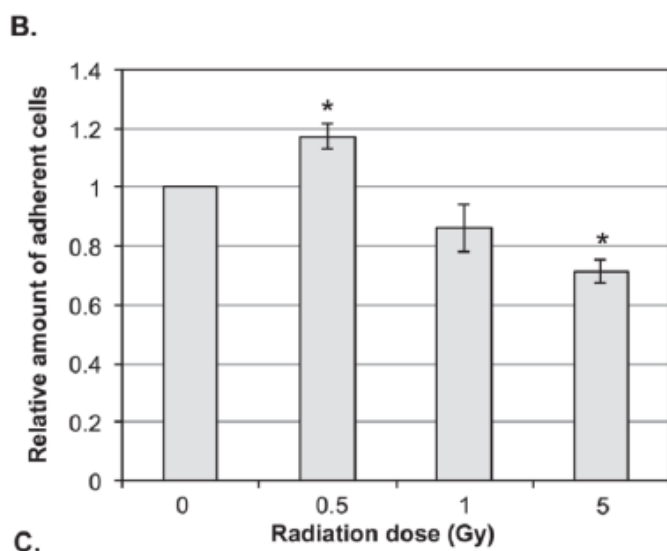
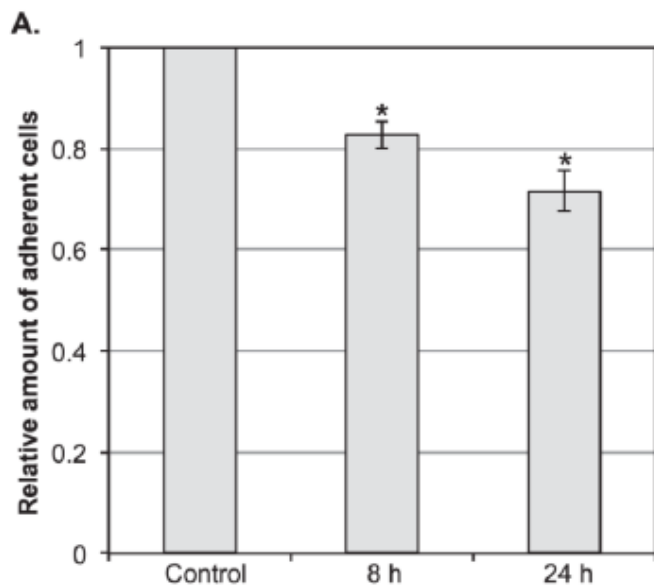


Figure 3.2 Adhesion of irradiated RAW264.7 cells to VCAM-1 under flow conditions.

Cell numbers were counted after trypan blue staining and adjusted to 5×10^6 /mL. The cells were perfused over the chamber coated with VCAM-1 at a physiological stress of 1.2 dynes/cm^2 . Relative amount of adherent cells were determined after 5 min perfusion. (A) RAW264.7 cells were irradiated with 5 Gy and the cell adhesion was analyzed at 8 h and 24 h post-irradiation. (B) RAW264.7 cells were irradiated with 0.5 Gy, 1 Gy or 5 Gy. The cell adhesion was analyzed at 24 h post-irradiation. (C) Percentage of cell death was determined by trypan blue staining at 24 h post-irradiation. Data shown are the means \pm SD from three independent experiments. *: $p < 0.05$ versus control.

The IR-altered avidity of RAW264.7 cells to VCAM-1 is ROS-dependent.

Since IR has been shown to generate free radicals, which play a significant role in regulating cells signaling after irradiation [162], we examined the extent of the effect of N-Acetyl-L-cysteine (L-NAC), a free radical scavenger, on the adhesion of RAW264.7 cells perfused over VCAM-1-coated chamber under the flow condition as described above. Our data showed that the avidities of L-NAC-treated RAW264.7 cells to VCAM-1 were reduced approximately 46% with no statistical differences among sham, 0.5 or 5.0 Gy of IR (Fig 3.3A).

Analysis of the surface expression of VLA-4 integrin indicated that neither $\alpha 4$ nor $\beta 1$ integrin on RAW264.7 cells surface was affected by the L-NAC treatment (Fig 3.3B, 3.3C). These results suggested that the IR-altered avidity of RAW264.7 cells involves free radicals, but does not involve the cell surface expression of VLA-4 integrin.

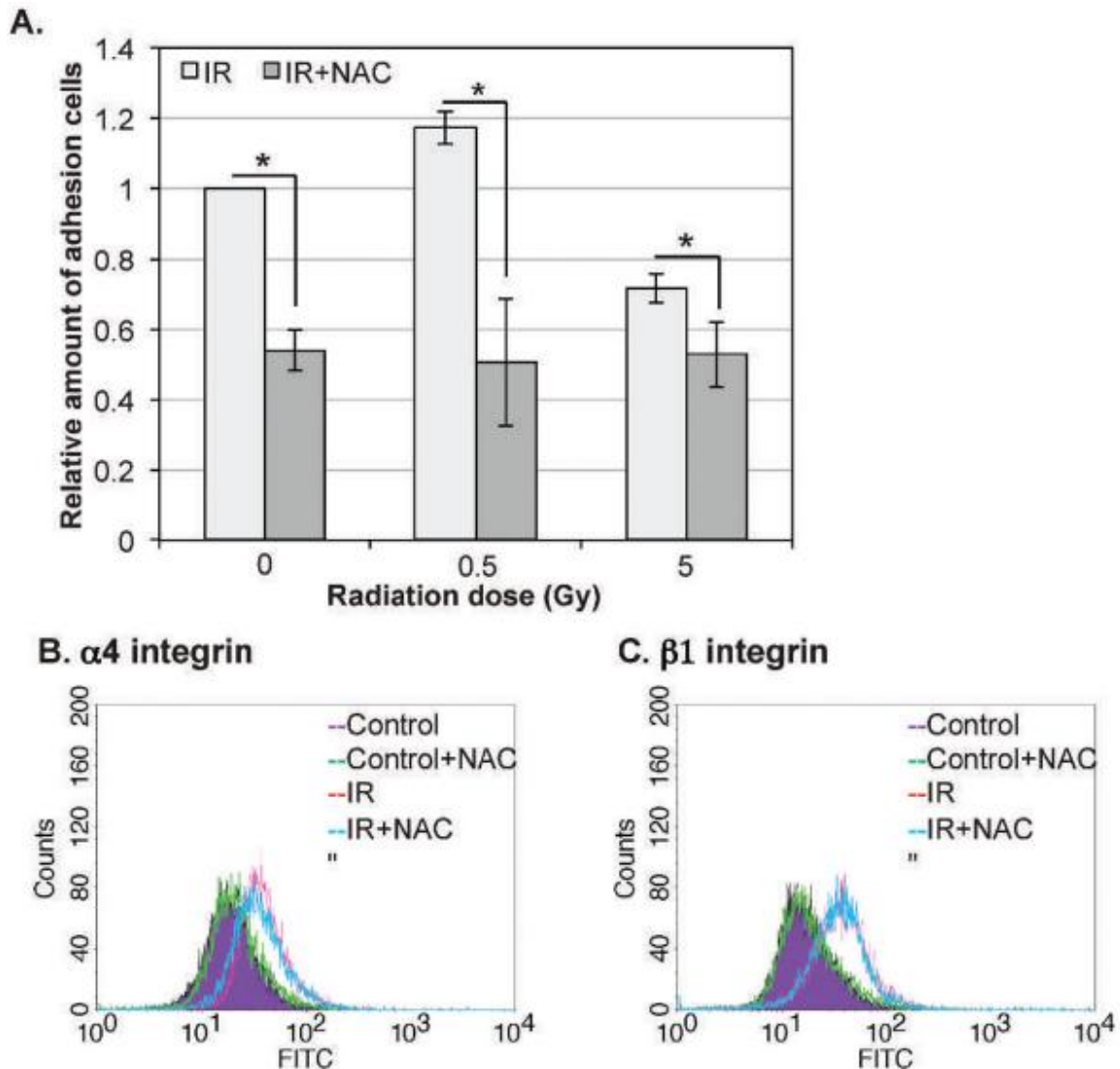


Figure 3.3 Effect of L-NAC on VLA-4 mediated adhesion of RAW264.7 cells under flow conditions. RAW264.7 cells were pretreated with 20 mM L-NAC for 1 hour prior to 0.5 and 5 Gy gamma irradiation. At 24 h post-irradiation, cells were counted after trypan blue staining to reach the same concentration (5×10^6 /mL) and perfused over the flow chamber at a physiological stress of 1.2 dynes/cm^2 . (A) Relative amount of adherent cells after 5 min perfusion. Data shown are the means \pm SD from three independent experiments. *: $p < 0.05$. (B) Surface expression of $\alpha 4$ and (C) $\beta 1$ integrin was analyzed by flow cytometry at 24 h post-irradiation (5 Gy) in the presence or absence of L-NAC (20 mM).

To determine whether reactive oxygen species (ROS) exert a direct effect on VLA-4-mediated adhesion, we determined the extent of the effect of exogenous H₂O₂ on the avidity of RAW264.7 cells to VCAM-1. Our data showed that after exogenous H₂O₂ treatment, the avidity of RAW264.7 cells to VCAM-1 was increased by 15.3±6.0% after treatment with 5 μM H₂O₂ and was then reduced by 20.3±7.6% or 46.0±11.4% after treatment with 50 μM or 100 μM H₂O₂, respectively, at 0.5 h post-treatment (Fig 3.4). These data further indicate that of adhesion of RAW264.7 cells to VCAM-1 is ROS-dependent and follows a bell-shaped dose response.

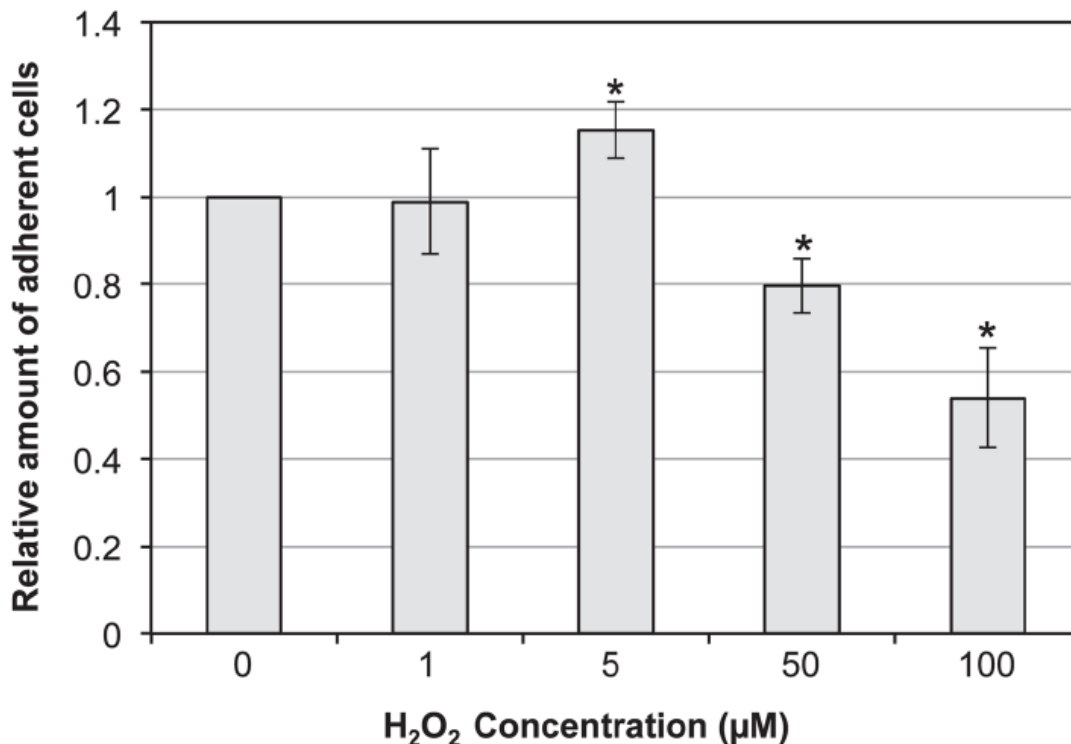


Figure 3.4 H₂O₂ regulates avidity of VLA-4 in RAW264.7 cells under flow conditions.

Cells were treated with 1 µM, 5 µM, 50 µM and 100 µM H₂O₂ and harvested after 30 min incubation. Cells were counted after trypan blue staining and adjusted to 5x10⁶/mL. Then the cells were perfused over the chamber coated with VCAM-1 at a shear stress of 1.2 dynes/cm². Cells adhered to the chamber were counted after 5 min perfusion. Data shown are the means ± SD from three independent experiments. *: *p*<0.05 versus 0 µM.

Discussion

While the biological effect of IR on adhesion molecules of endothelial cells has been studied [163-166], little is known regarding the contributions of irradiated monocytes/macrophages to radiotherapy-associated side effects. Macrophages are known as radio-resistant leukocytes that can bear high doses of IR [167]. Previous work has shown that indicated that ICAM-1 and LFA-1 on alveolar macrophages increased one week after IR [168]. However, the early

response (within 24 h) of monocytes/macrophages to IR in contributing to their avidity to endothelial cells has not been well characterized. Therefore, in this study, we first determined the extent of the effects of IR on the expression and surface localization of VLA-4 ($\alpha4\beta1$) integrin, the major integrin that mediates the adhesion between monocytes/macrophages and endothelial cells [151, 153]. Our data indicated that the surface levels of both $\alpha4$ and $\beta1$ integrins were increased. However, while the total expression of $\alpha4$ integrin was increased, $\beta1$ integrin was not changed at 24 h postirradiation (5 Gy) (Fig 3.1). The results suggested that IR induces translocation of $\beta1$ integrin to the surface of macrophages. However, further investigation indicated that the increased surface VLA-4 was not correlated to an increased avidity of RAW264.7 cells to VCAM-1, the ligand of VLA-4 (Fig 3.1 vs. 3.2). The results suggested that conformation change of integrin, which has been shown to play an important role in cell adhesion [169-173], may be a major contributor for IR-induced alternation of cell adhesion. A dose-dependent analysis of the response of RAW264.7 cells to IR revealed that the avidity between RAW264.7 cells and VCAM-1 was increased with a relatively lower dose (0.5 Gy) and reduced with relatively higher dose (1-5 Gy) of IR (Fig 3.2B). The reduction of the avidity was not likely due to cell death after IR because the percentage of reduced avidity was much higher than the percentage of reduced viability of the cells (Fig 3.2B vs. 3.2C). These results suggested that factor(s) other than VLA-4 were involved in regulation of the avidity of RAW264.7 cells. While our data indicated that the avidity between

RAW264.7 cells and VCAM-1 was increased after 0.5 Gy IR and decreased after 5 Gy IR, it does not suggest that a lower dose radiation is worse than a higher dose for IR-induced atherosclerosis, since a high dose of IR has been shown to induce the expression of various adhesion molecules on endothelial cells [174].

It has been previously reported that sulfhydryl groups involved in VLA-4 mediated adhesion can be regulated by ROS [175]. The VLA-4-mediated avidity of human leukocytes to VCAM-1 was increased and then decreased in response to a treatment of 5-100 μM exogenous H_2O_2 [175]. Considering that IR generates ROS in a dose dependent manner [42], we determined the effect of L-NAC, a free radical scavenger, on the IR-induced and VLA-4-mediated avidity of RAW264.7 cells. Our data demonstrated that, while the treatment of L-NAC did not alter the surface expression of VLA-4 in the presence or absence of IR (Fig 3.3B, C), it reduced the avidity of RAW264.7 cells to VCAM-1 to a similar level, regardless of whether the cells were treated or not treated with a higher or lower dose of IR (Fig 3.3A). The L-NAC-decreased avidity of the cells is likely due to the reduction of ROS rather than reactive nitrogen species (RNS), since IR didn't induce the expression of any one of the three nitric oxide synthases in RAW264.7 cells (data not shown). To further investigate the role of ROS in regulation of VLA-4-mediated adhesion, the avidity of RAW264.7 cells, which were treated with 1 to 100 μM exogenous H_2O_2 , were determined by parallel flow chamber assay. Consistent with our expectation, the avidity of RAW264.7 cells to VCAM-1 in responding to exogenous H_2O_2 was increased at lower (5 μM)

H₂O₂ and then decreased at higher (50-100 μM) H₂O₂ (Fig 3.4), which is similar to what has been documented in human leukocytes [175]. In conclusion, we have demonstrated that VLA-4-mediated adhesion of RAW264.7 cells to VCAM-1 is altered by IR under flow conditions, in which ROS plays a key role according to its concentration. In addition, a basal level of ROS is required for maintaining normal affinity between VLA-4 and VCAM-1.

CHAPTER 4 : THE ROLES OF PERK AND EIF2A PHOSPHORYLATION IN IONIZING RADIATION-INDUCED G₂/M ARREST

Introduction

Ionizing radiation (IR) has been one of the cornerstones of cancer treatment [30]. To detect and respond to IR-induced DNA damage, especially lethal DNA double-strand breaks (DSBs), is crucial for cell fate determination [37, 38]. To prevent propagation of damaged DNA, cell cycle checkpoints are activated for necessary repair. In fact, ataxia telangiectasia mutated (ATM) is able to activate G₁ [176, 177], intra-S [178] and G₂ checkpoints [179] after quickly recognizing DSBs with the assistance of MRE11-RAD50-NBS1 (MRN) complex [180]. Failure to remove DNA damage before proceeding to mitosis may result in cell death [181].

Disruption of endoplasmic reticulum homeostasis and consequent accumulation of misfolded proteins can result from different environmental challenges, including inhibition of glycosylation, glucose deprivation, hypoxia, and disturbance of calcium influx [182-184]. Protein misfolding is known to trigger an adaptive mechanism called unfolded protein response (UPR), which is transduced by PKR-like endoplasmic reticulum kinase (PERK), activating transcription factor 6 (ATF6) and inositol-requiring enzyme 1 (IRE1) [182, 185]. In UPR, PERK acts as an eukaryotic translation initiation factor-2 α (eIF2 α) kinase which attenuates translation to reduce ER stress [90, 186]. Interestingly, emerging evidence in recent years has unveiled a link between IR and ER stress.

Activation of PERK and corresponding eIF2 α phosphorylation has been observed in human umbilical vascular cells after exposure to IR (15 Gy) [187]. In caspase-3/7 double-knockout mouse embryonic fibroblasts, IR (5 Gy) was shown to induce significant autophagy which was mediated by PERK and eIF2 α phosphorylation [188]. IR-induced ER stress is believed to promote autophagy when caspase pathways are deficient [189]. Other studies show that drug-induced ER stress help to overcome radiation resistance of cancer cells [190, 191].

In terms of cell cycle regulation, previous work revealed that PERK-mediated translation inhibition of cyclin D1 played a central role in UPR-dependent G₁ arrest [192]. The researchers also found that eIF2 α phosphorylation instead of PERK is indispensable in tunicamycin-induced G₁ arrest because another eIF2 α kinase, general control nonderepressible 2 (GCN2), may still contribute to eIF2 α phosphorylation [193]. In addition to a direct repression of cyclin D1 after eIF2 α phosphorylation in response to UPR, altered interactions of ribosomal proteins and subsequent degradation of p53 are also involved in G₁ arrest [194]. Although PERK and eIF2 α phosphorylation were linked in UPR-dependent cell cycle arrest, their roles in IR-induced cell cycle arrest remains unclear. Herein, we report that basal level of eIF2 α phosphorylation contributes to IR-induced G₂/M arrest. Furthermore, inhibition of ATM sensitized PERK knockout cells to IR-induced G₂/M arrest, which does not rely on eIF2 α phosphorylation. Our findings advance the understanding of IR-

induced ER stress and cell cycle arrest, which may shed light on the causes of radiation resistance.

Materials and Methods

Cell Culture

Mouse embryonic fibroblast (MEF), including wild type (MEF^{WT}), PERK knockout (MEF^{PERK^{-/-}}) and eIF2 α S51A mutant (MEF^{A/A}) were kindly provided by Dr. Randal Kaufman, Sanford Burnham Prebys Medical Discovery Institute, La Jolla, CA). MEF cells were grown in Dulbecco's Modified Eagle Medium (DMEM) (Corning, Manassas, VA) supplemented with 10% fetal bovine serum (Atlanta Biologicals, Lawrenceville, GA) and 1% penicillin/streptomycin.

Cell Survival Analysis

Cell survival after IR was measured using FITC Annexin V Apoptosis Detection Kit (BD Biosciences) per the manufacturer's instructions. Cells were irradiated with 10 Gy and maintained in the incubator for 72 h. Briefly, cells were harvested and washed with cold PBS twice before resuspension in 1X binding buffer. Concentration of cell suspension was adjusted to 1×10^6 cells/mL. Then 0.1 mL of cell suspension was transferred to a 1.5 mL centrifuge tube. Cells were incubated with 5 μ L propidium iodide (PI) staining solution and FITC Annexin V for 15 min and another 0.4 mL binding buffer was added before analysis. Signal of FITC and PI was analyzed on a BD CSampler flow cytometer (BD Biosciences).

Cell Growth Analysis

To measure cell growth after IR, 2×10^5 cells were seeded in 100 mm dishes to grow overnight before IR. 0 h was defined as the time when cells were irradiated with 10 Gy. Cells were harvested and counted at 0 h, 24 h and 48 h.

Western Blotting

Cells were harvested and washed with cold PBS. 2% NP-40 buffer mixed with protease inhibitor was added to cell pellets. Samples were incubated on ice for 15 min and then centrifuged at 13,200 rpm at 4 °C for 10 min. Supernatant was collected and quantified by DC protein assay kit (Bio-Rad Laboratories). Equal amount of proteins were loaded and separated in 15% SDS-PAGE resolving gel and then transferred to a nitrocellulose membrane (Pall, Port Washington, NY). 5% non-fat milk in Tris-buffered saline with Tween (TBS-T) was used to block the membrane for 1 h at room temperature. The membrane was then probed with anti-eIF2 α (sc-11386, Santa Cruz Biotechnology), anti-phospho-eIF2A (44728G, Invitrogen), anti-phospho-cdc2 (Tyr15) (4539, Cell Signaling), anti- β -actin (sc-47778, Santa Cruz Biotechnology) overnight on a rotary shaker at 4°C. Membranes were washed three times with Tris-buffered saline with Tween (TBS-T) before incubating with HRP-conjugated secondary antibodies for 0.5 h at room temperature. After being washed with TBS-T three times and with TBS twice, blots were developed using West Pico Supersignal chemiluminescent substrate (Pierce, Rockford, IL).

Cell Cycle Analysis

Appropriate amount of cells were seeded in 100 mm dishes according to numbers below. For cells tested as control and 6 h post radiation, 5.6×10^5 cells were seeded. For cells used at 24 h post radiation, 2.2×10^5 MEF^{WT}, 3.7×10^5 MEF^{PERK^{-/-}} and MEF^{A/A} cells were seeded to grow overnight before IR. Fewer cells were seeded if additional 24 h serum starvation was needed. At each time point after IR, cells were harvested and then washed by PBS. Cells were resuspended in 1.5 mL ice cold PBS and then added dropwise to equal amount of cold absolute ethanol while vortexing. Samples were stored at -20°C for at least 12 hours for fixation. Before staining, cells were centrifuged for 10 min at 4°C to remove ethanol and washed with cold PBS once. Cells were resuspended in 1 mL fresh buffer (0.2 mg/mL DNase free RNase A, 0.1% Triton X-100 in PBS, 20 $\mu\text{g}/\text{mL}$ propidium iodide) and incubated at room temperature for 30 min. Signals were acquired on a FACSAria Special Order Research Product flowcytometer (BD Biosciences). FlowJo VX (FlowJo LLC, Ashland, OR) was used for cell cycle analysis.

Statistical Analysis

Student's t-test was applied to compare the difference between groups. Only $p < 0.05$ was considered to be statistically significant.

Results

IR induces eIF2 α phosphorylation and causes growth inhibition of MEFs

Studies in recent years have revealed that IR regulates eIF2 α phosphorylation [187, 188], the critical switch of translation. Therefore, first we compared the level of eIF2 α phosphorylation in MEF^{WT}, MEF^{PERK^{-/-}} and MEF^{A/A} cells following radiation (10 Gy). There was no phosphorylation detected in MEF^{A/A} cells as expected due to its nonphosphorylatable eIF2 α (S51A mutant) (Fig 4.1). Significant eIF2 α phosphorylation was induced at 24 h after IR in wild type MEFs, while a slight increase can be observed at 1 h and 6 h. PERK has been shown to mediate IR-induced autophagy [188], and our data directly demonstrated the dominant role of PERK in IR-induced eIF2 α phosphorylation because there was almost no increase of phosphorylation during 24 h (Fig 4.1).

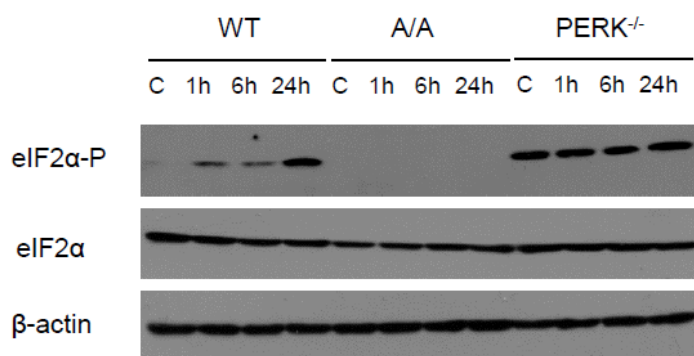


Figure 4.1 eIF2 α phosphorylation at 1 h, 6 h and 24 h following IR was measured by Western blot.

A representative image of 3 independent experiments is shown.

IR delivers energy to the cell directly, which slows cell growth and leads to cell death [33]. To determine the cell proliferation rate after radiation, cells were counted at 24 and 48 h. Significant inhibition of cell growth was seen in all MEFs postirradiation (Fig 4.2). MEF^{PERK^{-/-}} cells appeared to stop growing from 24 h while wild type MEFs continued to grow very slowly from 24 to 48 h after radiation. Although it is not statistically significant between 24 and 48 h following IR in MEF^{A/A} cells, it still showed increasing trend from 24 h (1.8 ± 0.2 -fold) to 48 h (2.7 ± 1.0 -fold) after treatment (Fig. 4.2). During the time course of 48 h, few floating cells were observed after IR. To confirm the effect of IR-induced cell death, we used Annexin V-FITC and PI double staining to assess cell survival at 72 h post IR. No significant increase of dead cells was detected (PI positive/ PI & Annexin V positive cells), which excluded the impact of cell death within 72 h after IR (Fig 4.3). These results suggested that IR (10Gy) inhibited cell proliferation but did not lead to significant cell death.

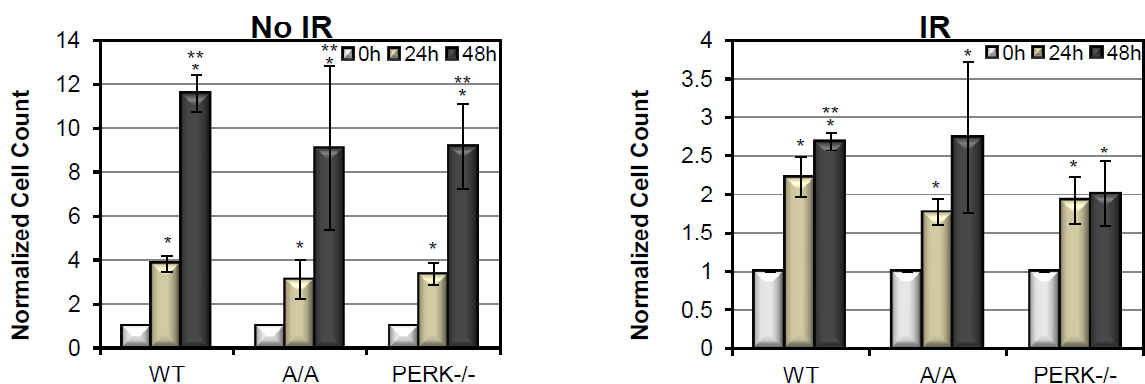


Figure 4.2 Cell growth was measured at 24 h and 48 h post irradiation. *, $p < 0.05$ versus control; **, $p < 0.05$ versus 24 h. The error bar represents \pm SD, $n=4$.

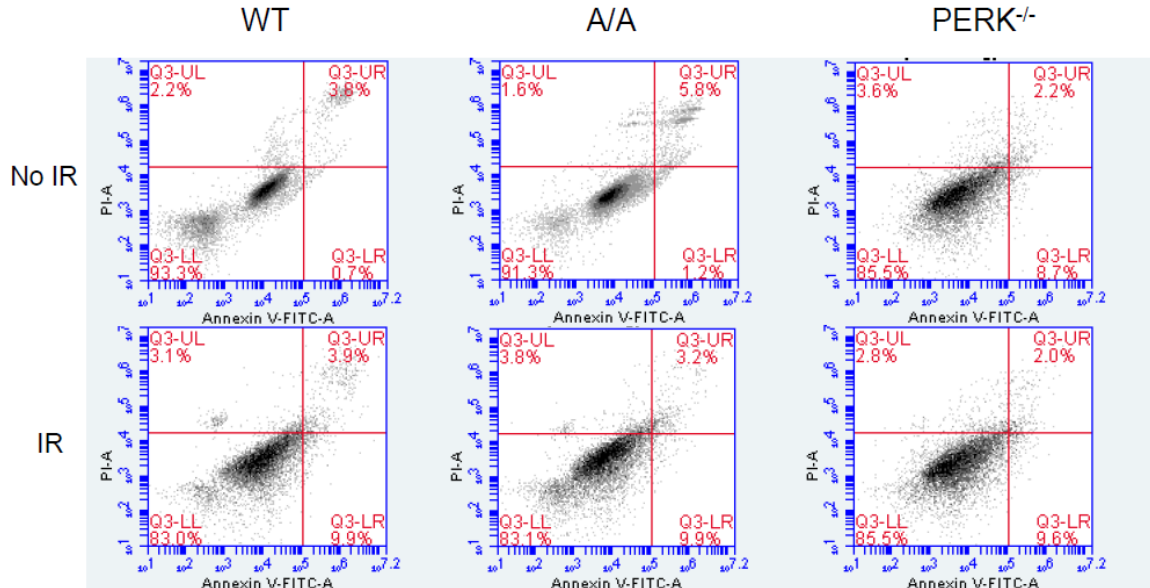


Figure 4.3 Cell death was evaluated by Annexin V-FITC and PI double staining at 72 h after IR. Representative images of 2 independent experiments are shown.

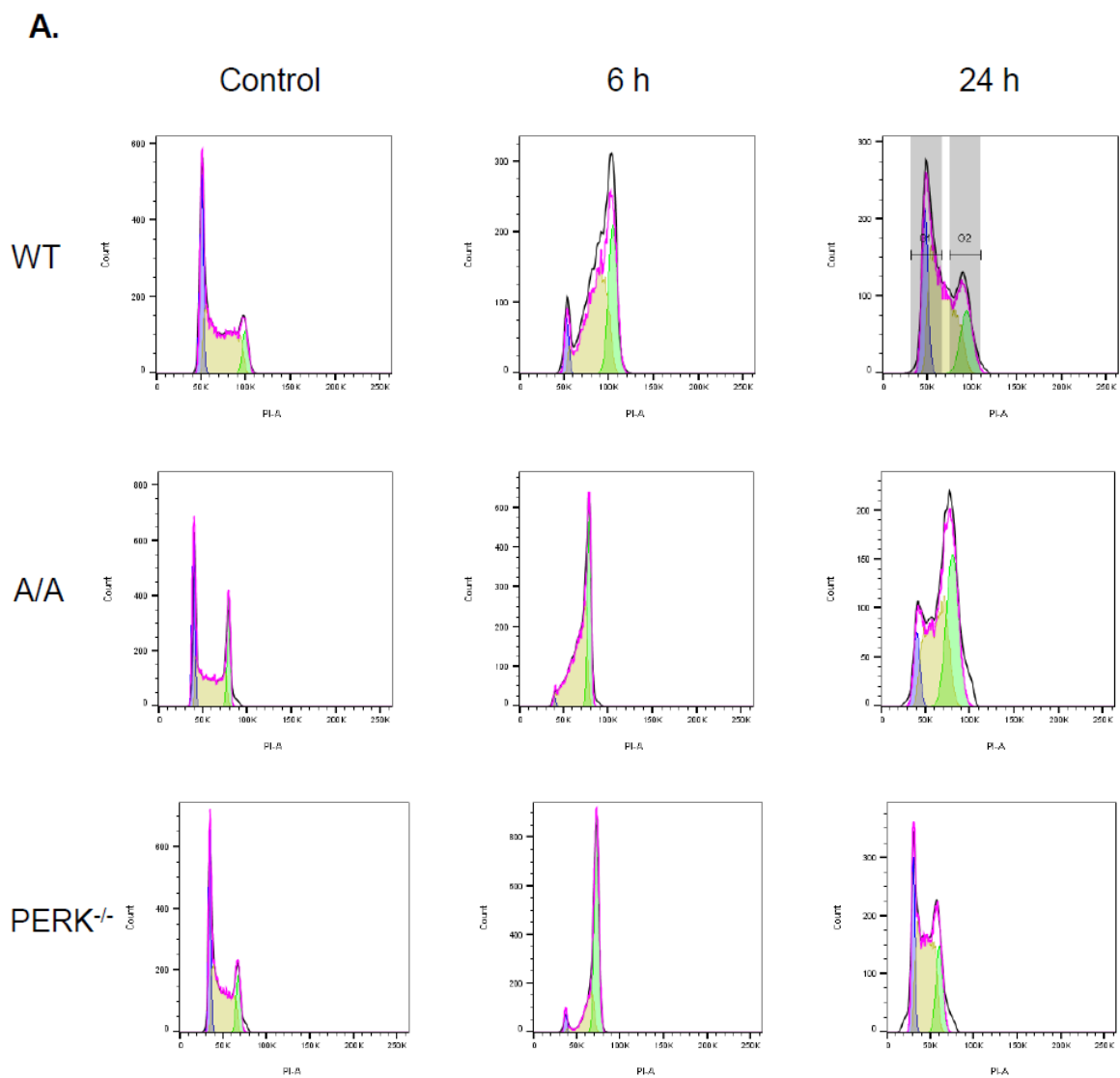
Abolishment of eIF2 α phosphorylation desensitizes MEF cells to IR-induced

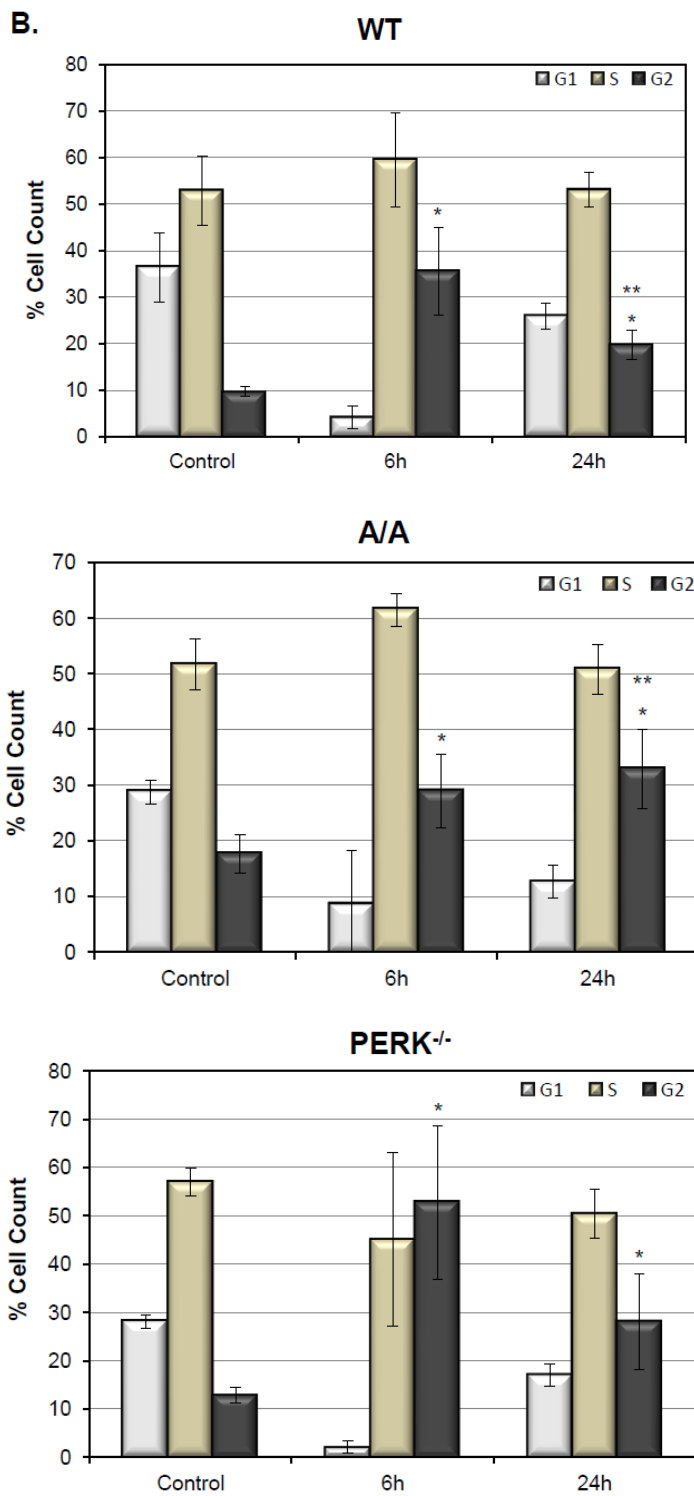
G₂/M arrest

Given that cell growth is inhibited due to delayed cell cycle, we examined cell cycle arrest in MEF^{WT}, MEF^{PERK^{-/-}} and MEF^{A/A} cells in response to IR (10 Gy). Our data showed that G₂/M arrest is the primary physiological effect within 24 h in all MEFs (Fig 4.4A, B). MEF^{WT} cells showed a sharp increase of G₂/M distribution at 6 h ($35.6 \pm 9.4\%$) and then partially recovered from G₂/M arrest at 24 h ($19.8 \pm 3.1\%$) after IR (Fig 4.4B). Similarly, MEF^{PERK^{-/-}} cells showed a greater response to IR at 6 h ($52.7 \pm 15.8\%$) although the decrease at 24 h ($28.1 \pm 9.9\%$) is not statistically significant. MEF^{A/A} cells showed less G₂/M arrest at 6 h ($28.9 \pm 6.7\%$) and did not change much at 24 h ($32.8 \pm 7.2\%$). When compared

to normal G₂ distribution, MEF^{WT} cells showed approximately a 3.7-fold and a 2-fold increase at 6 h and 24 h, respectively (Fig 4.4B). Similar fold change was also observed in MEF^{PERK^{-/-}} cells. Interestingly, MEF^{A/A} cells, which has a higher normal G₂/M distribution compared to MEF^{WT}, MEF^{PERK^{-/-}} cells, showed only approximately a 1.6-fold and a 1.9-fold increase at 6 h and 24 h, respectively (Fig 4.4B).

Because only significant G₂/M arrest was induced after IR, we next examined phosphorylation of cdc2 in MEFs. Cdc2/CyclinB complex needs to be active to drive G₂/M transition. The inhibition of cdc2/CyclinB complex is achieved by phosphorylation of cdc2 at Tyr15 and Thr14 [195, 196]. Our data showed that phosphorylation of cdc2 was induced at 6 h and recovered at 24 h following IR in MEF^{WT}, MEF^{PERK^{-/-}} and MEF^{A/A} cells despite their different basal level (Fig 4.4C).





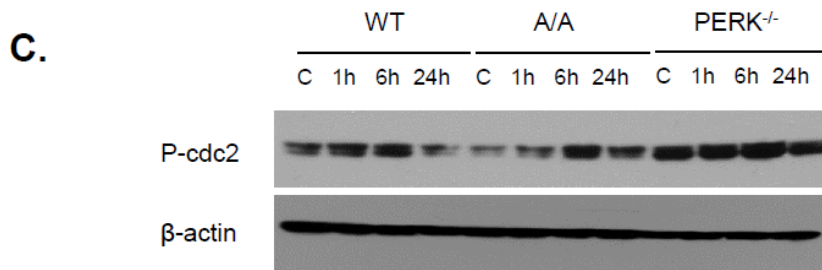


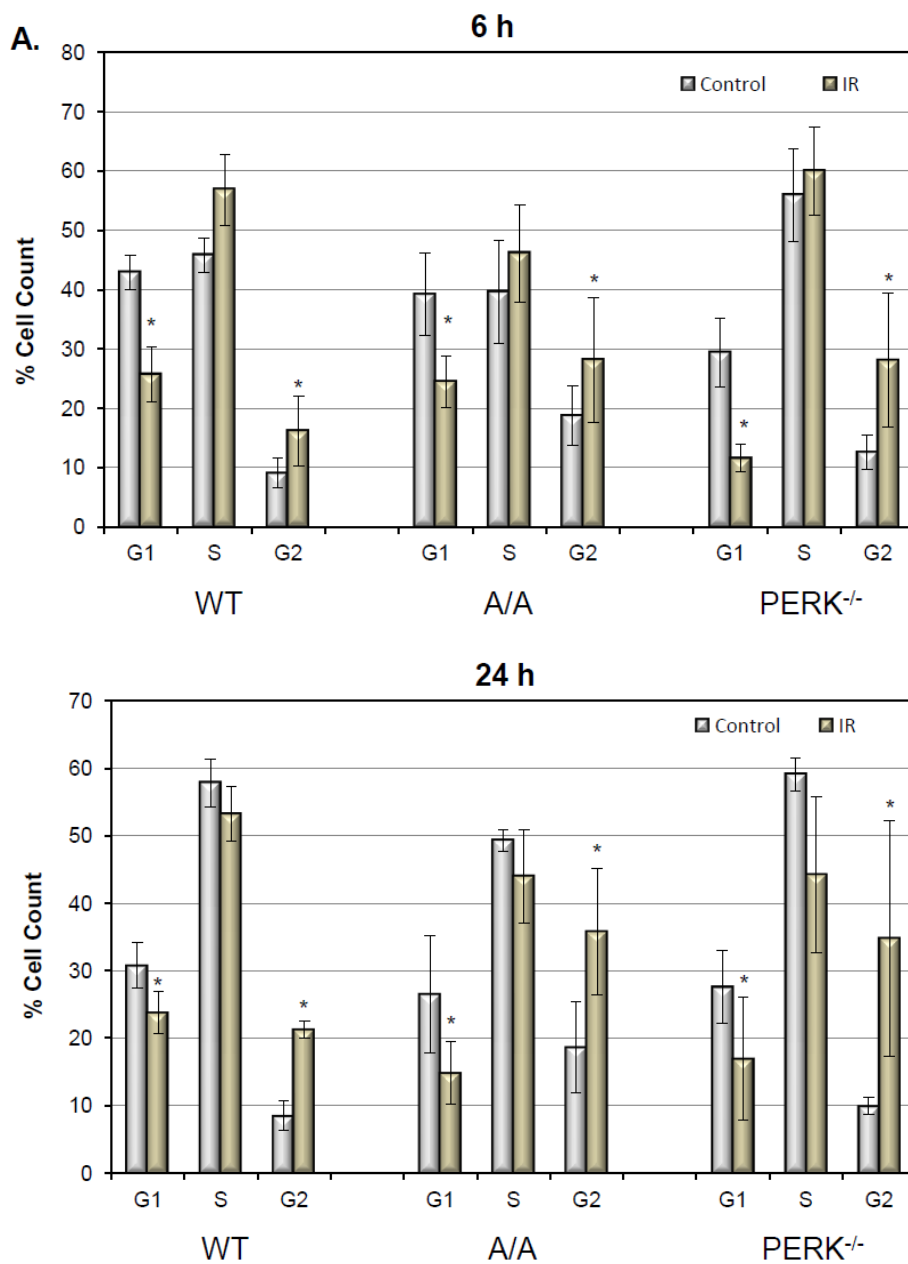
Figure 4.4 IR-induced G₂/M arrest in MEFs. MEF^{WT}, MEF^{PERK^{-/-}} and MEF^{A/A} cells were irradiated with 10 Gy.

Cell cycle was analyzed at 6 h and 24 h following IR. (A) Representative images of 4 independent experiments are shown. (B) Quantification of IR-induced G₂/M arrest. The error bar represents \pm SD, n=4. *, $p < 0.05$ versus control; **, $p < 0.05$ versus 6 h. (C) Phospho-cdc2 after IR was assessed by Western blot. A representative image of 3 independent experiments is shown.

These data indicated that G₂/M arrest still occurred without PERK. In addition, the cells became less sensitized to IR-induced G₂/M arrest in the absence of basal level of eIF2 α phosphorylation. This partially explained the reason for growth inhibition in MEF^{WT} and MEF^{PERK^{-/-}} cells and less impact on MEF^{A/A} cells after IR.

To provide supplementary evidence, we also tested IR-induced G₂/M arrest after serum starvation, which usually leads to accumulation in the G1 phase [197]. Compared to its control after serum starvation, MEF^{WT} still showed increased level of eIF2 α phosphorylation at 24 h postirradiation (Fig 4.5B). The effect of serum starvation alone on cell cycle distribution was not significant compared to cells in complete medium (Fig 4.5A vs Fig 4.4B). Our data showed that serum starvation blunted IR-induced G₂/M arrest in MEF^{WT} ($16.2 \pm 5.2\%$) and MEF^{PERK^{-/-}} cells ($28.1 \pm 11.3\%$) but not in MEF^{A/A} cells ($28.2 \pm 10.5\%$) at early time (6 h) compared to cells without serum starvation (Fig 4.4B vs. Fig 4.5),

which adds evidence to the central role of basal level of eIF2 α phosphorylation in regulation of IR-induced G₂/M arrest.



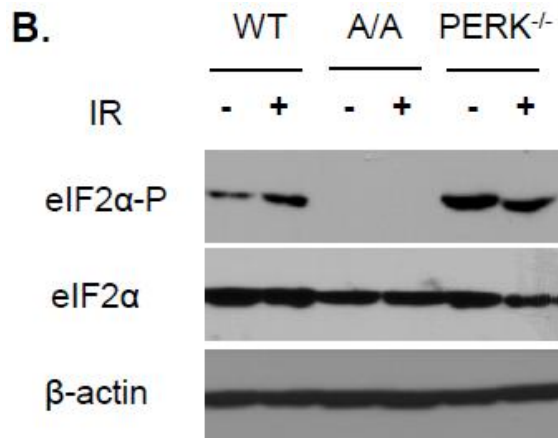
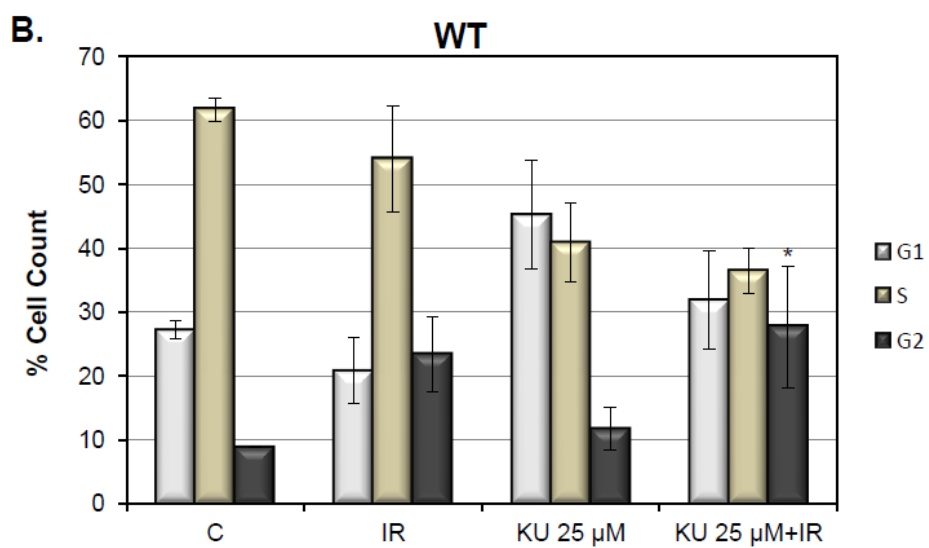
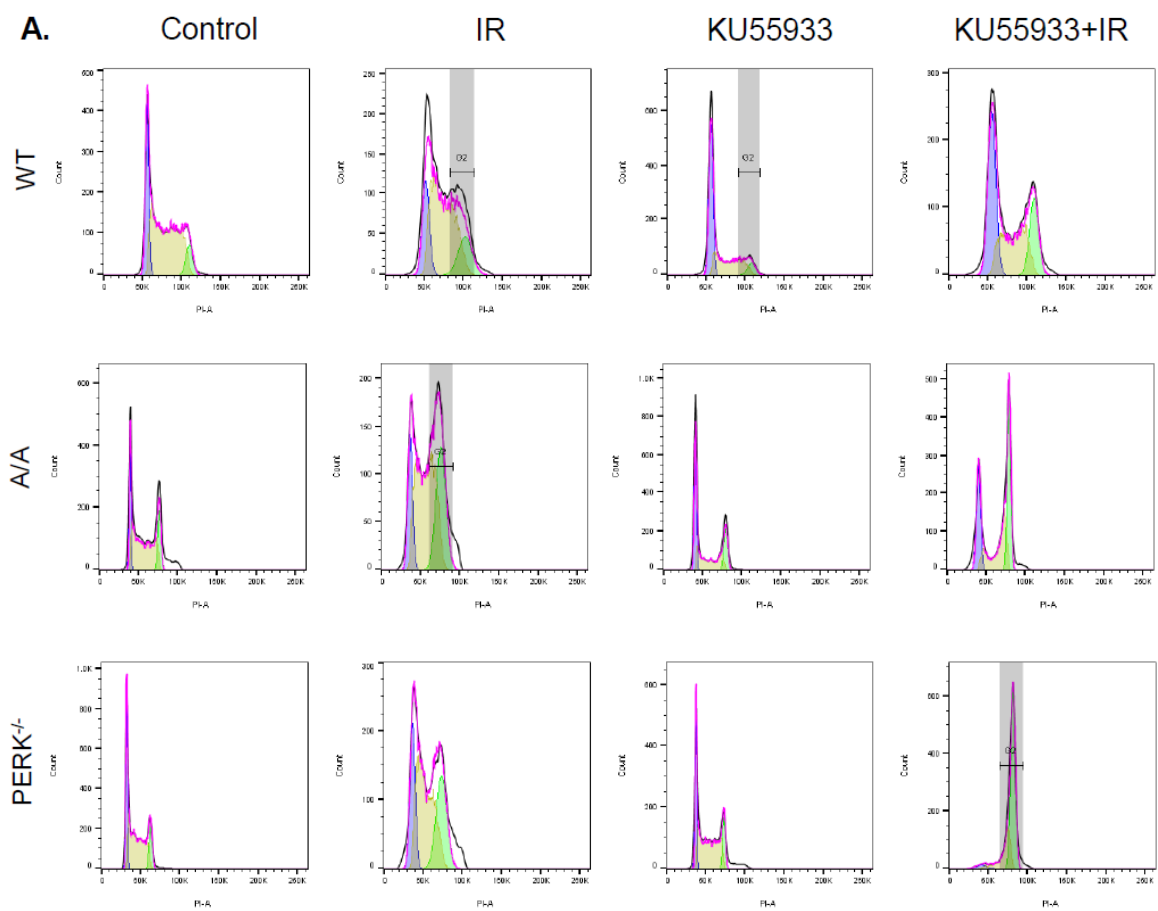


Figure 4.5 Cells were irradiated with 10 Gy after serum starvation for 24 h. (A) Cell cycle was analyzed at 6 h and 24 h following IR. *, $p < 0.05$ versus control. The error bar represents \pm SD, $n=4$. (B) After serum starvation, eIF2 α phosphorylation at 24 h following IR was measured by Western blot. A representative image of 3 independent experiments is shown.

Inhibition of ATM sensitizes MEF^{PERK^{-/-}} cells to IR-induced G₂/M arrest

Fast recognition of DSBs relies on ATM which initiates G₂/M arrest

[179][180]. To determine the role of ATM in regulating G₂/M arrest, a widely used ATM inhibitor KU55933 was combined with IR [198][199]. Our data showed that blockade of ATM did not change IR-induced G₂/M arrest in MEF^{WT} and MEF^{A/A} cells at 24 h after IR (Fig 4.6A, B). Interestingly, a sharp increase of cells caught in G₂/M phase (from $15.8 \pm 4.9\%$ to $64.9 \pm 4.6\%$) was found in MEF^{PERK^{-/-}} cells treated with both IR and KU55933 (Fig. 4.6B). This data indicated that inhibition of ATM amplified IR-induced G₂/M arrest in the absence of PERK.



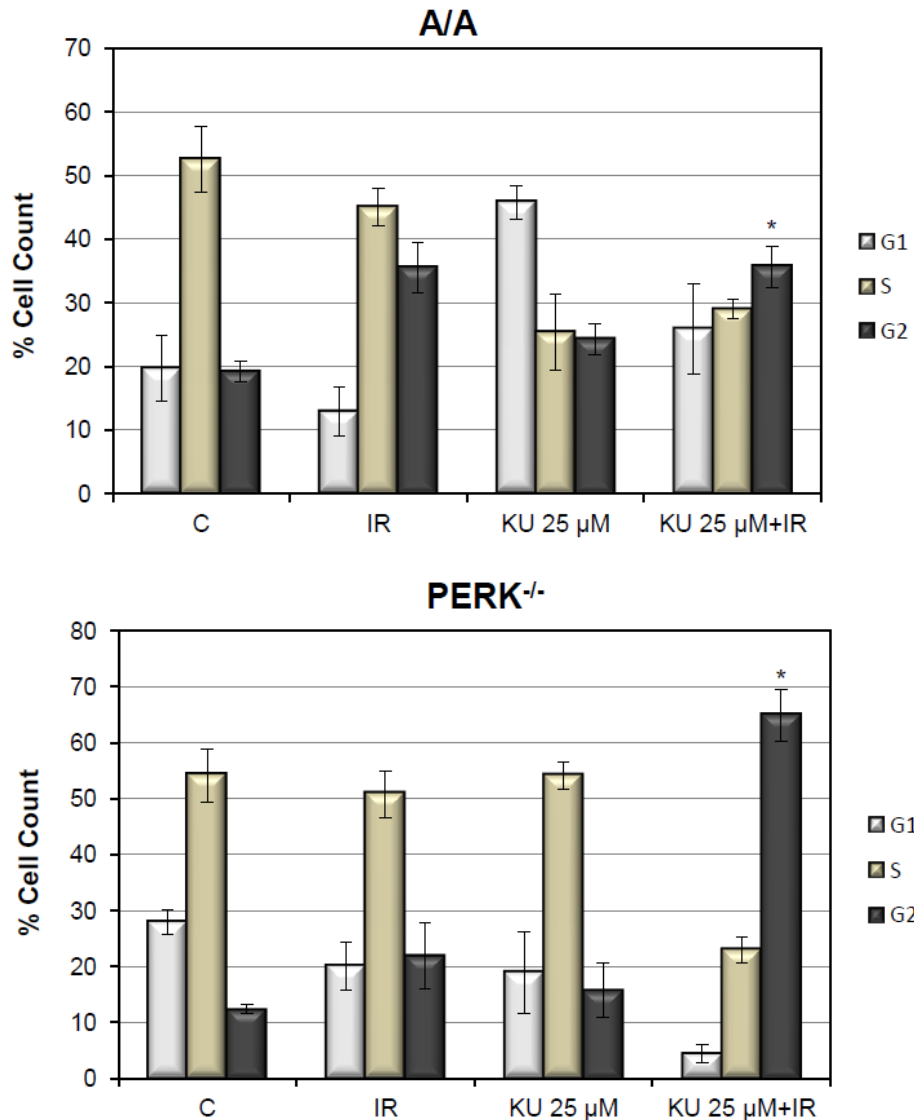


Figure 4.6 Effect of KU55933 on IR-induced G₂/M arrest in MEFs. MEF^{WT}, MEF^{PERK^{-/-}} and MEF^{A/A} cells were treated with 25 μ M KU55933 for 2 h prior to IR (10 Gy). Cell cycle was evaluated at 24 h following IR. (A) Representative images of 3 independent experiments are shown. (B) Quantification of IR-induced G₂/M arrest. *, $p < 0.05$ versus KU 25 μ M treatment. The error bar represents \pm SD, $n=3$.

Discussion

Cell cycle checkpoints are regulated by multiple signaling pathways and the overall effect can be complicated. Both PERK and eIF2 α phosphorylation are involved in different stages of cell cycle. For regulation of G₁ arrest, eIF2 α kinases, PERK and GCN2, were shown to suppress translation of cyclin D1 through eIF2 α phosphorylation [193]. For regulation of G₂/M arrest, research in recent years has indicated that translation inhibition during ER stress activated CHK1 and caused early G₂/M arrest, which was ATM-independent and more significant in p53 mutant cells [200]. Although ER stress is able to regulate both G₁ and G₂ phases, it should be noted that drug-induced UPR (e.g. tunicamycin/thapsigargin) does not lead to significant DSBs compared to IR. Therefore, ATM signaling may override signaling pathways in drug-induced UPR. For instance, the above mentioned CHK1 could be more activated by IR-induced DNA damage and contribute to IR-induced G₂/M arrest [201], which may have longer and stronger effect compared to drug-induced UPR alone.

In our experiment, only IR-induced G₂/M arrest was observed in MEF^{WT}, MEF^{PERK^{-/-}} and MEF^{A/A} cells (Fig 4.4). In terms of eIF2 α phosphorylation, IR-induced eIF2 α phosphorylation was primarily mediated by PERK (Fig 4.1). In terms of IR-induced cell cycle arrest, MEF^{PERK^{-/-}} cells showed slightly higher percentage in G₂/M compared to wild type (Fig 4.4). However, the effect of PERK knockout on G₂/M arrest was much less significant compared to nonphosphorylatable eIF2 α , suggesting that the basal level of eIF2 α

phosphorylation weighed more than PERK itself in regulating IR-induced G₂/M arrest when ATM is intact.

It is well established that ATM is able to regulate G₁, S and G₂ checkpoints through activating various substrates [202][203]. The ATM inhibitor KU55933 has been shown as a potential radiation sensitizer because it can inhibit DNA damage repair [204][205]. One of these reports showed that G₂/M arrest was partially abrogated by KU55933 [206]. However, our data showed that IR-induced G₂/M accumulation was not reduced after ATM inhibition in MEF^{WT} and MEF^{A/A} cells. Moreover, ATM inhibition sensitized IR-induced G₂/M arrest in MEF^{PERK^{-/-}} cells, showing the potential of ATM independent G₂/M arrest (Fig 4.6B). This exaggerated G₂/M arrest is consistent with an early study of KU55933 [199]. This effect of sensitization might be due to insufficient transition of cells from S phase back to G₁ phase postirradiation, which was further attributed to defective S-phase checkpoints in cells lacking of ATM [207]. Cells with mutant Nbs1, a key regulator of S-phase checkpoint showed prolonged G₂/M arrest after IR. In view of the result that the sensitization of IR-induced G₂/M arrest after ATM inhibition was only seen in MEF^{PERK^{-/-}} but not in MEF^{WT} or MEF^{A/A} cells, it suggests that PERK might be involved in maintaining S-phase checkpoints. Actually, significant cell death was observed when MEF^{PERK^{-/-}} cells were treated with 0.5 mM hydroxyurea (HU) for 24 h (Fig 4.7). Given that HU is a classic ribonucleotide reductase inhibitor to reduce deoxyribonucleotide precursors, which activates S phase checkpoints [208], and forces cells to accumulate at

G1/S boundary or S phase [209, 210], the S-phase checkpoints might be somehow defective in $MEF^{PERK^{-/-}}$ cells, because they failed to arrest in early S phase and tend to undergo cell death.

In summary, a model was proposed in Fig 4.8. Both conventional ATM signaling and eIF2 α phosphorylation contribute to IR-induced G₂/M arrest. PERK mediates IR-induced eIF2 α phosphorylation while eIF2 α phosphorylation promotes G₂/M arrest. When ATM is blocked, PERK is necessary to limit G₂/M arrest in response to IR.

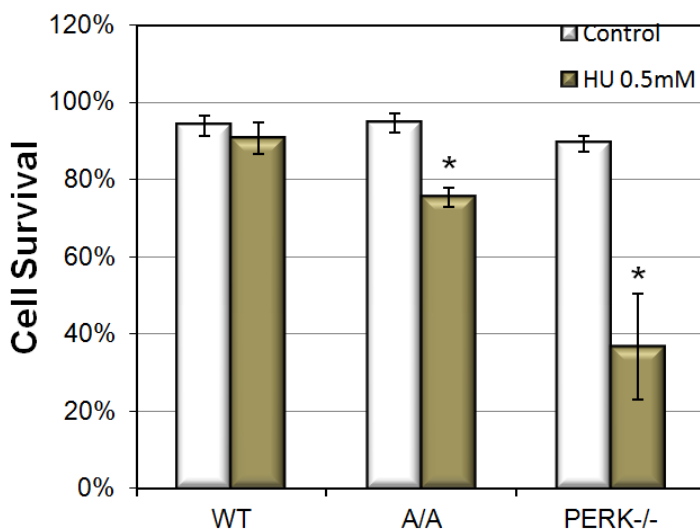


Figure 4.7 MEFs were treated with hydroxyurea (0.5 mM) for 24 h. Cells were then stained with trypan blue. Cells that excluded trypan blue were counted as living cells. *, $p < 0.05$ versus control. The error bar represents \pm SD, $n=3$.

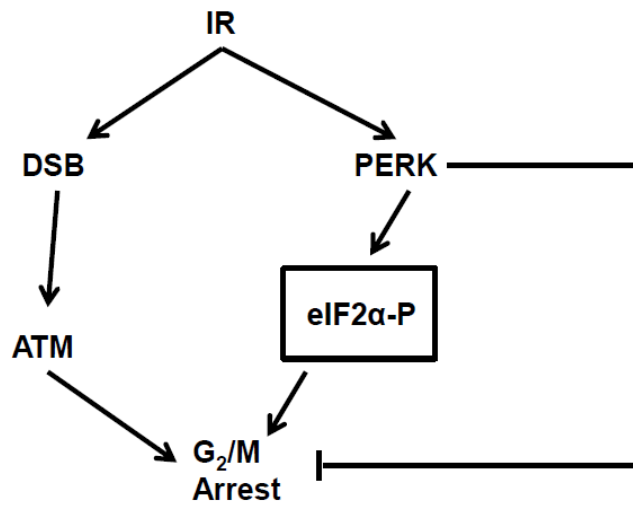


Figure 4.8 A proposed model for the roles of PERK and eIF2 α phosphorylation in the regulation of IR-induced G₂/M arrest.

CHAPTER 5 : FUTURE DIRECTIONS

Given that IR-induced ROS play an important role in DNA damage, further investigation involving ROS is needed. In addition to ROS directly generated from radiolysis, the dysfunction of mitochondria cannot be ignored. On one hand, mitochondria dysfunction may increase the ROS level as a delayed effect of IR. On the other hand, it is also involved in DNA damage response, showing its role in the postirradiation adaptive mechanism [211]. As a matter of fact, studies have connected mitochondria with cell cycle progression, both of which are highly dynamic processes [212-214]. The complex of cyclin B1 and CDK1 has been shown to regulate manganese superoxide dismutase (MnSOD), which is required to limit free radicals produced in mitochondria [215].

Previous data in Chapter 4 has shown that eIF2 α phosphorylation contributes to IR-induced cell cycle arrest. Interestingly, our preliminary data showed a possible link between eIF2 α phosphorylation and mitochondria function (Fig 5.1). Although oxygen consumption rate (OCR) of MEF^{AA} and MEF^{WT} cells are similar at basal level, the potential of mitochondria in MEF^{AA} cell is much higher. Therefore, to determine the ROS level and mitochondria function postirradiation might be helpful to explore the correlation between ROS and IR-induced cell cycle arrest or DNA damage. If significant differences of ROS/OCAR can be found, N-Acetyl-L-cysteine (L-NAC) will be used as an antioxidant to reduce ROS level after IR and the role of ROS in IR-induced G₂/M arrest will be assessed.

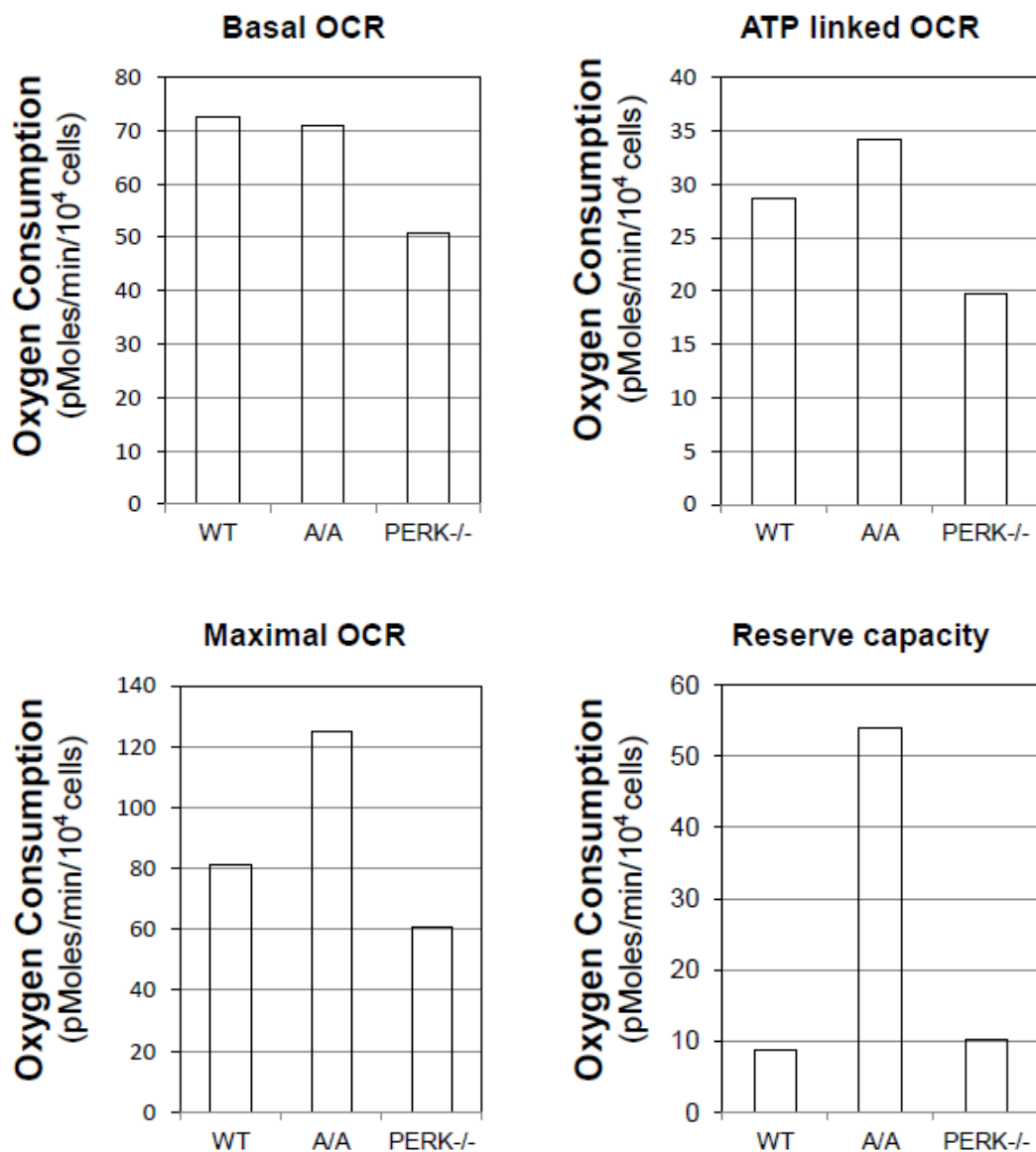


Figure 5.1 Oxygen consumption rate (OCR) of MEFs. 3.5×10^4 cells/well were seeded on a 24-well plate. OCR was measured by a Seahorse XF24 Extracellular Flux analyzer using the protocol of mitochondria stress test. The result was normalized to cell numbers after counting cells right after the test. Preliminary data shown here was from a single test.

REFERENCES

1. Tamkun, J.W., et al., *Structure of integrin, a glycoprotein involved in the transmembrane linkage between fibronectin and actin*. Cell, 1986. **46**(2): p. 271-82.
2. Barczyk, M., S. Carracedo, and D. Gullberg, *Integrins*. Cell Tissue Res, 2010. **339**(1): p. 269-80.
3. Takagi, J., *Structural basis for ligand recognition by integrins*. Curr Opin Cell Biol, 2007. **19**(5): p. 557-64.
4. Pan, L., et al., *Research advances on structure and biological functions of integrins*. Springerplus, 2016. **5**(1): p. 1094.
5. Campbell, I.D. and M.J. Humphries, *Integrin structure, activation, and interactions*. Cold Spring Harb Perspect Biol, 2011. **3**(3).
6. Lee, J.O., et al., *Two conformations of the integrin A-domain (I-domain): a pathway for activation?* Structure, 1995. **3**(12): p. 1333-40.
7. Hogervorst, F., et al., *Cloning and sequence analysis of beta-4 cDNA: an integrin subunit that contains a unique 118 kd cytoplasmic domain*. EMBO J, 1990. **9**(3): p. 765-70.
8. Dickinson, C.D., et al., *Crystal structure of the tenth type III cell adhesion module of human fibronectin*. J Mol Biol, 1994. **236**(4): p. 1079-92.
9. Humphries, J.D., A. Byron, and M.J. Humphries, *Integrin ligands at a glance*. J Cell Sci, 2006. **119**(Pt 19): p. 3901-3.

10. Knight, C.G., et al., *Identification in collagen type I of an integrin alpha2 beta1-binding site containing an essential GER sequence*. J Biol Chem, 1998. **273**(50): p. 33287-94.
11. Huttenlocher, A. and A.R. Horwitz, *Integrins in cell migration*. Cold Spring Harb Perspect Biol, 2011. **3**(9): p. a005074.
12. Ginsberg, M.H., A. Partridge, and S.J. Shattil, *Integrin regulation*. Curr Opin Cell Biol, 2005. **17**(5): p. 509-16.
13. Calderwood, D.A., et al., *The phosphotyrosine binding-like domain of talin activates integrins*. J Biol Chem, 2002. **277**(24): p. 21749-58.
14. Partridge, A.W., et al., *Transmembrane domain helix packing stabilizes integrin alphaIIb beta3 in the low affinity state*. J Biol Chem, 2005. **280**(8): p. 7294-300.
15. Luo, B.H., et al., *Disrupting integrin transmembrane domain heterodimerization increases ligand binding affinity, not valency or clustering*. Proc Natl Acad Sci U S A, 2005. **102**(10): p. 3679-84.
16. Burbach, B.J., et al., *T-cell receptor signaling to integrins*. Immunol Rev, 2007. **218**: p. 65-81.
17. Green, C.E., et al., *Shear-dependent capping of L-selectin and P-selectin glycoprotein ligand 1 by E-selectin signals activation of high-avidity beta2-integrin on neutrophils*. J Immunol, 2004. **172**(12): p. 7780-90.

18. Legate, K.R., S.A. Wickstrom, and R. Fassler, *Genetic and cell biological analysis of integrin outside-in signaling*. *Genes Dev*, 2009. **23**(4): p. 397-418.
19. Calalb, M.B., T.R. Polte, and S.K. Hanks, *Tyrosine phosphorylation of focal adhesion kinase at sites in the catalytic domain regulates kinase activity: a role for Src family kinases*. *Mol Cell Biol*, 1995. **15**(2): p. 954-63.
20. Thomas, J.W., et al., *SH2- and SH3-mediated interactions between focal adhesion kinase and Src*. *J Biol Chem*, 1998. **273**(1): p. 577-83.
21. Slack-Davis, J.K., et al., *PAK1 phosphorylation of MEK1 regulates fibronectin-stimulated MAPK activation*. *J Cell Biol*, 2003. **162**(2): p. 281-91.
22. Roovers, K., et al., *Alpha5beta1 integrin controls cyclin D1 expression by sustaining mitogen-activated protein kinase activity in growth factor-treated cells*. *Mol Biol Cell*, 1999. **10**(10): p. 3197-204.
23. Desgrosellier, J.S. and D.A. Cheresh, *Integrins in cancer: biological implications and therapeutic opportunities*. *Nat Rev Cancer*, 2010. **10**(1): p. 9-22.
24. Danen, E.H., et al., *Emergence of alpha 5 beta 1 fibronectin- and alpha v beta 3 vitronectin-receptor expression in melanocytic tumour progression*. *Histopathology*, 1994. **24**(3): p. 249-56.

25. Hsu, M.Y., et al., *Adenoviral gene transfer of beta3 integrin subunit induces conversion from radial to vertical growth phase in primary human melanoma*. Am J Pathol, 1998. **153**(5): p. 1435-42.
26. Nip, J., et al., *Human melanoma cells derived from lymphatic metastases use integrin alpha v beta 3 to adhere to lymph node vitronectin*. J Clin Invest, 1992. **90**(4): p. 1406-13.
27. Chambers, A.F., et al., *Critical steps in hematogenous metastasis: an overview*. Surg Oncol Clin N Am, 2001. **10**(2): p. 243-55, vii.
28. Klemke, M., et al., *High affinity interaction of integrin alpha4beta1 (VLA-4) and vascular cell adhesion molecule 1 (VCAM-1) enhances migration of human melanoma cells across activated endothelial cell layers*. J Cell Physiol, 2007. **212**(2): p. 368-74.
29. Liang, S. and C. Dong, *Integrin VLA-4 enhances sialyl-Lewisx/a-negative melanoma adhesion to and extravasation through the endothelium under low flow conditions*. Am J Physiol Cell Physiol, 2008. **295**(3): p. C701-7.
30. Barton, M.B., et al., *Estimating the demand for radiotherapy from the evidence: a review of changes from 2003 to 2012*. Radiother Oncol, 2014. **112**(1): p. 140-4.
31. Delaney, G.P. and M.B. Barton, *Evidence-based estimates of the demand for radiotherapy*. Clin Oncol (R Coll Radiol), 2015. **27**(2): p. 70-6.
32. Tyldesley, S., et al., *Estimating the need for radiotherapy for patients with prostate, breast, and lung cancers: verification of model estimates of need*

- with radiotherapy utilization data from British Columbia*. Int J Radiat Oncol Biol Phys, 2011. **79**(5): p. 1507-15.
33. Cadet, J., et al., *Hydroxyl radicals and DNA base damage*. Mutat Res, 1999. **424**(1-2): p. 9-21.
 34. Ward, J.F., *DNA damage produced by ionizing radiation in mammalian cells: identities, mechanisms of formation, and reparability*. Prog Nucleic Acid Res Mol Biol, 1988. **35**: p. 95-125.
 35. Rothkamm, K. and M. Lobrich, *Evidence for a lack of DNA double-strand break repair in human cells exposed to very low x-ray doses*. Proc Natl Acad Sci U S A, 2003. **100**(9): p. 5057-62.
 36. Nikjoo, H., et al., *Track structure in radiation biology: theory and applications*. Int J Radiat Biol, 1998. **73**(4): p. 355-64.
 37. Lips, J. and B. Kaina, *DNA double-strand breaks trigger apoptosis in p53-deficient fibroblasts*. Carcinogenesis, 2001. **22**(4): p. 579-85.
 38. Steel, G.G., *The case against apoptosis*. Acta Oncol, 2001. **40**(8): p. 968-75.
 39. Caputo, F., R. Vegliante, and L. Ghibelli, *Redox modulation of the DNA damage response*. Biochem Pharmacol, 2012. **84**(10): p. 1292-306.
 40. Azzam, E.I., J.P. Jay-Gerin, and D. Pain, *Ionizing radiation-induced metabolic oxidative stress and prolonged cell injury*. Cancer Lett, 2012. **327**(1-2): p. 48-60.

41. Russo, M.T., et al., *Different DNA repair strategies to combat the threat from 8-oxoguanine*. *Mutat Res*, 2007. **614**(1-2): p. 69-76.
42. Leach, J.K., et al., *Ionizing radiation-induced, mitochondria-dependent generation of reactive oxygen/nitrogen*. *Cancer Res*, 2001. **61**(10): p. 3894-901.
43. Muntean, D.M., et al., *The Role of Mitochondrial Reactive Oxygen Species in Cardiovascular Injury and Protective Strategies*. *Oxid Med Cell Longev*, 2016. **2016**: p. 8254942.
44. Boveris, A., E. Cadenas, and A.O. Stoppani, *Role of ubiquinone in the mitochondrial generation of hydrogen peroxide*. *Biochem J*, 1976. **156**(2): p. 435-44.
45. Yamamori, T., et al., *Ionizing radiation induces mitochondrial reactive oxygen species production accompanied by upregulation of mitochondrial electron transport chain function and mitochondrial content under control of the cell cycle checkpoint*. *Free Radic Biol Med*, 2012. **53**(2): p. 260-70.
46. Thariat, J., et al., *Image-guided radiation therapy for muscle-invasive bladder cancer*. *Nat Rev Urol*, 2012. **9**(1): p. 23-9.
47. Jerezek-Fossa, B.A., et al., *Primary focal prostate radiotherapy: Do all patients really need whole-prostate irradiation?* *Crit Rev Oncol Hematol*, 2016. **105**: p. 100-11.
48. Hafner, M.F. and J. Debus, *Radiotherapy for Colorectal Cancer: Current Standards and Future Perspectives*. *Visc Med*, 2016. **32**(3): p. 172-7.

49. Hickey, B.E., et al., *Fraction size in radiation therapy for breast conservation in early breast cancer*. Cochrane Database Syst Rev, 2016. **7**: p. CD003860.
50. Ohri, N., et al., *Radiotherapy for Hepatocellular Carcinoma: New Indications and Directions for Future Study*. J Natl Cancer Inst, 2016. **108**(9).
51. Zheng, Y., M.T. Jaklitsch, and R. Bueno, *Neoadjuvant Therapy in Non-Small Cell Lung Cancer*. Surg Oncol Clin N Am, 2016. **25**(3): p. 567-84.
52. De Bari, B., et al., *Hypofractionated radiotherapy in pancreatic cancer: Lessons from the past in the era of stereotactic body radiation therapy*. Crit Rev Oncol Hematol, 2016. **103**: p. 49-61.
53. Li, H., X. Wu, and X. Cheng, *Advances in diagnosis and treatment of metastatic cervical cancer*. J Gynecol Oncol, 2016. **27**(4): p. e43.
54. Pivonello, R., et al., *Cushing's disease: the burden of illness*. Endocrine, 2016.
55. Eberlein, B. and T. Biedermann, *To remember: Radiotherapy - a successful treatment for early Dupuytren's disease*. J Eur Acad Dermatol Venereol, 2016.
56. Petrelli, F., et al., *Surveillance or Adjuvant Treatment With Chemotherapy or Radiotherapy in Stage I Seminoma: A Systematic Review and Meta-Analysis of 13 Studies*. Clin Genitourin Cancer, 2015. **13**(5): p. 428-34.

57. O'Rorke, M.A., et al., *The value of adjuvant radiotherapy on survival and recurrence in triple-negative breast cancer: A systematic review and meta-analysis of 5507 patients*. *Cancer Treat Rev*, 2016. **47**: p. 12-21.
58. Chen, X., et al., *Radiotherapy can improve the disease-free survival rate in triple-negative breast cancer patients with T1-T2 disease and one to three positive lymph nodes after mastectomy*. *Oncologist*, 2013. **18**(2): p. 141-7.
59. Mak, R.H., et al., *Bladder preservation: optimizing radiotherapy and integrated treatment strategies*. *BJU Int*, 2008. **102**(9 Pt B): p. 1345-53.
60. Redmond, K.J., et al., *Postoperative Stereotactic Body Radiation Therapy (SBRT) for Spine Metastases: A Critical Review to Guide Practice*. *Int J Radiat Oncol Biol Phys*, 2016. **95**(5): p. 1414-28.
61. Chow, E., et al., *Palliation of bone metastases: a survey of patterns of practice among Canadian radiation oncologists*. *Radiother Oncol*, 2000. **56**(3): p. 305-14.
62. Bae, J.S., et al., *Laryngeal edema after radiotherapy in patients with squamous cell carcinomas of the larynx and hypopharynx*. *Oral Oncol*, 2012. **48**(9): p. 853-8.
63. Bray, F.N., et al., *Acute and Chronic Cutaneous Reactions to Ionizing Radiation Therapy*. *Dermatol Ther (Heidelb)*, 2016. **6**(2): p. 185-206.
64. Omolehinwa, T.T. and S.O. Akintoye, *Chemical and Radiation-Associated Jaw Lesions*. *Dent Clin North Am*, 2016. **60**(1): p. 265-77.

65. Dennis, K., et al., *International patterns of practice in the management of radiation therapy-induced nausea and vomiting*. Int J Radiat Oncol Biol Phys, 2012. **84**(1): p. e49-60.
66. Barbarino, R., et al., *Fatigue in patients undergoing radiation therapy: an observational study*. Minerva Med, 2013. **104**(2): p. 185-91.
67. Stewart, J.R. and L.F. Fajardo, *Radiation-induced heart disease. Clinical and experimental aspects*. Radiol Clin North Am, 1971. **9**(3): p. 511-31.
68. Darby, S.C., et al., *Long-term mortality from heart disease and lung cancer after radiotherapy for early breast cancer: prospective cohort study of about 300,000 women in US SEER cancer registries*. Lancet Oncol, 2005. **6**(8): p. 557-65.
69. Martinou, M. and A. Gaya, *Cardiac complications after radical radiotherapy*. Semin Oncol, 2013. **40**(2): p. 178-85.
70. Yusuf, S.W., et al., *Radiation-related heart and vascular disease*. Future Oncol, 2015. **11**(14): p. 2067-76.
71. Taylor, C.W., et al., *Cardiac dose from tangential breast cancer radiotherapy in the year 2006*. Int J Radiat Oncol Biol Phys, 2008. **72**(2): p. 501-7.
72. Stewart, F.A., et al., *Ionizing radiation accelerates the development of atherosclerotic lesions in ApoE^{-/-} mice and predisposes to an inflammatory plaque phenotype prone to hemorrhage*. Am J Pathol, 2006. **168**(2): p. 649-58.

73. Hoving, S., et al., *Single-dose and fractionated irradiation promote initiation and progression of atherosclerosis and induce an inflammatory plaque phenotype in ApoE(-/-) mice*. *Int J Radiat Oncol Biol Phys*, 2008. **71**(3): p. 848-57.
74. Mancuso, M., et al., *Acceleration of atherogenesis in ApoE-/- mice exposed to acute or low-dose-rate ionizing radiation*. *Oncotarget*, 2015. **6**(31): p. 31263-71.
75. Kreuzer, M., et al., *Low-dose ionising radiation and cardiovascular diseases--Strategies for molecular epidemiological studies in Europe*. *Mutat Res Rev Mutat Res*, 2015. **764**: p. 90-100.
76. Little, M.P., et al., *A systematic review of epidemiological associations between low and moderate doses of ionizing radiation and late cardiovascular effects, and their possible mechanisms*. *Radiat Res*, 2008. **169**(1): p. 99-109.
77. Borghini, A., et al., *Ionizing radiation and atherosclerosis: current knowledge and future challenges*. *Atherosclerosis*, 2013. **230**(1): p. 40-7.
78. Bhattacharya, S. and A. Asaithamby, *Ionizing radiation and heart risks*. *Semin Cell Dev Biol*, 2016. **58**: p. 14-25.
79. Voeltz, G.K., M.M. Rolls, and T.A. Rapoport, *Structural organization of the endoplasmic reticulum*. *EMBO Rep*, 2002. **3**(10): p. 944-50.
80. English, A.R., N. Zurek, and G.K. Voeltz, *Peripheral ER structure and function*. *Curr Opin Cell Biol*, 2009. **21**(4): p. 596-602.

81. Schroder, M. and R.J. Kaufman, *ER stress and the unfolded protein response*. Mutat Res, 2005. **569**(1-2): p. 29-63.
82. Zhao, L. and S.L. Ackerman, *Endoplasmic reticulum stress in health and disease*. Curr Opin Cell Biol, 2006. **18**(4): p. 444-52.
83. Xu, C., B. Bailly-Maitre, and J.C. Reed, *Endoplasmic reticulum stress: cell life and death decisions*. J Clin Invest, 2005. **115**(10): p. 2656-64.
84. Sano, R. and J.C. Reed, *ER stress-induced cell death mechanisms*. Biochim Biophys Acta, 2013. **1833**(12): p. 3460-70.
85. Lee, J.H., et al., *Induction of the unfolded protein response and cell death pathway in Alzheimer's disease, but not in aged Tg2576 mice*. Exp Mol Med, 2010. **42**(5): p. 386-94.
86. He, B., *Viruses, endoplasmic reticulum stress, and interferon responses*. Cell Death Differ, 2006. **13**(3): p. 393-403.
87. Lee, G.S., et al., *The calcium-sensing receptor regulates the NLRP3 inflammasome through Ca²⁺ and cAMP*. Nature, 2012. **492**(7427): p. 123-7.
88. Cimellaro, A., et al., *Role of endoplasmic reticulum stress in endothelial dysfunction*. Nutr Metab Cardiovasc Dis, 2016. **26**(10): p. 863-71.
89. Bu, Y. and J.A. Diehl, *PERK Integrates Oncogenic Signaling and Cell Survival During Cancer Development*. J Cell Physiol, 2016. **231**(10): p. 2088-96.

90. Rozpedek, W., et al., *The Role of the PERK/eIF2alpha/ATF4/CHOP Signaling Pathway in Tumor Progression During Endoplasmic Reticulum Stress*. *Curr Mol Med*, 2016. **16**(6): p. 533-44.
91. Novoa, I., et al., *Feedback inhibition of the unfolded protein response by GADD34-mediated dephosphorylation of eIF2alpha*. *J Cell Biol*, 2001. **153**(5): p. 1011-22.
92. Ma, Y. and L.M. Hendershot, *Delineation of a negative feedback regulatory loop that controls protein translation during endoplasmic reticulum stress*. *J Biol Chem*, 2003. **278**(37): p. 34864-73.
93. Kimata, Y., et al., *A role for BiP as an adjustor for the endoplasmic reticulum stress-sensing protein Ire1*. *J Cell Biol*, 2004. **167**(3): p. 445-56.
94. Yoshida, H., et al., *XBP1 mRNA is induced by ATF6 and spliced by IRE1 in response to ER stress to produce a highly active transcription factor*. *Cell*, 2001. **107**(7): p. 881-91.
95. Yoshida, H., et al., *XBP1 is critical to protect cells from endoplasmic reticulum stress: evidence from Site-2 protease-deficient Chinese hamster ovary cells*. *Cell Struct Funct*, 2006. **31**(2): p. 117-25.
96. Yoshida, H., et al., *pXBP1(U) encoded in XBP1 pre-mRNA negatively regulates unfolded protein response activator pXBP1(S) in mammalian ER stress response*. *J Cell Biol*, 2006. **172**(4): p. 565-75.

97. Ye, J., et al., *ER stress induces cleavage of membrane-bound ATF6 by the same proteases that process SREBPs*. Mol Cell, 2000. **6**(6): p. 1355-64.
98. Hynes, R.O., *Integrins: bidirectional, allosteric signaling machines*. Cell, 2002. **110**(6): p. 673-87.
99. Bianchi-Smiraglia, A., S. Paesante, and A.V. Bakin, *Integrin beta5 contributes to the tumorigenic potential of breast cancer cells through the Src-FAK and MEK-ERK signaling pathways*. Oncogene, 2012. **32**(25): p. 3049-3058.
100. Lafrenie, R.M., et al., *Up-regulated biosynthesis and expression of endothelial cell vitronectin receptor enhances cancer cell adhesion*. Cancer Res, 1992. **52**(8): p. 2202-8.
101. Aoudjit, F. and K. Vuori, *Integrin signaling in cancer cell survival and chemoresistance*. Chemother Res Pract, 2012. **2012**: p. 283181.
102. Eke, I., E. Dickreuter, and N. Cordes, *Enhanced radiosensitivity of head and neck squamous cell carcinoma cells by beta1 integrin inhibition*. Radiother Oncol, 2012. **104**(2): p. 235-42.
103. Askari, J.A., et al., *Linking integrin conformation to function*. J Cell Sci, 2009. **122**(Pt 2): p. 165-70.
104. Arnaout, M.A., S.L. Goodman, and J.P. Xiong, *Structure and mechanics of integrin-based cell adhesion*. Curr Opin Cell Biol, 2007. **19**(5): p. 495-507.

105. Seales, E.C., et al., *A protein kinase C/Ras/ERK signaling pathway activates myeloid fibronectin receptors by altering beta1 integrin sialylation*. J Biol Chem, 2005. **280**(45): p. 37610-5.
106. Seales, E.C., et al., *Hypersialylation of beta1 integrins, observed in colon adenocarcinoma, may contribute to cancer progression by up-regulating cell motility*. Cancer Res, 2005. **65**(11): p. 4645-52.
107. Shaikh, F.M., et al., *Tumor cell migration and invasion are regulated by expression of variant integrin glycoforms*. Exp Cell Res, 2008. **314**(16): p. 2941-50.
108. Seales, E.C., et al., *Ras oncogene directs expression of a differentially sialylated, functionally altered beta1 integrin*. Oncogene, 2003. **22**(46): p. 7137-45.
109. Bull, C., et al., *Targeting aberrant sialylation in cancer cells using a fluorinated sialic acid analog impairs adhesion, migration, and in vivo tumor growth*. Mol Cancer Ther, 2013. **12**(10): p. 1935-46.
110. Ada, G.L., E.L. French, and P.E. Lind, *Purification and properties of neuraminidase from Vibrio cholerae*. J Gen Microbiol, 1961. **24**: p. 409-25.
111. Cassidy, J.T., G.W. Jourdian, and S. Roseman, *The sialic acids. VI. Purification and properties of sialidase from Clostridium perfringens*. J Biol Chem, 1965. **240**(9): p. 3501-6.

112. St Geme, J.W., 3rd, *The HMW1 adhesin of nontypeable Haemophilus influenzae recognizes sialylated glycoprotein receptors on cultured human epithelial cells*. *Infect Immun*, 1994. **62**(9): p. 3881-9.
113. Corfield, A.P., et al., *The specificity of viral and bacterial sialidases for alpha(2-3)- and alpha(2-6)-linked sialic acids in glycoproteins*. *Biochim Biophys Acta*, 1983. **744**(2): p. 121-6.
114. Saito, M., K. Sugano, and Y. Nagai, *Action of Arthrobacter ureafaciens sialidase on sialoglycolipid substrates. Mode of action and highly specific recognition of the oligosaccharide moiety of ganglioside GM1*. *J Biol Chem*, 1979. **254**(16): p. 7845-54.
115. Shibuya, N., et al., *The elderberry (Sambucus nigra L.) bark lectin recognizes the Neu5Ac(alpha 2-6)Gal/GalNAc sequence*. *J Biol Chem*, 1987. **262**(4): p. 1596-601.
116. Taatjes, D.J., et al., *Elderberry bark lectin--gold techniques for the detection of Neu5Ac (alpha 2,6) Gal/GalNAc sequences: applications and limitations*. *Histochem J*, 1988. **20**(9): p. 478-90.
117. Cheng, H., et al., *Effects of nitric oxide-releasing nonsteroidal anti-inflammatory drugs (NONO-NSAIDs) on melanoma cell adhesion*. *Toxicol Appl Pharmacol*, 2012. **264**(2): p. 161-6.
118. Vercoutter-Edouart, A.S., et al., *Glycoproteomics and glycomics investigation of membrane N-glycosylproteins from human colon carcinoma cells*. *Proteomics*, 2008. **8**(16): p. 3236-56.

119. Kemmner, W., J. Morgenthaler, and R. Brossmer, *Alterations in cell surface carbohydrate composition of a human colon carcinoma cell line affect adhesion to extracellular matrix components*. *Biochimie*, 1992. **74**(1): p. 117-22.
120. Almaraz, R.T., et al., *Metabolic flux increases glycoprotein sialylation: implications for cell adhesion and cancer metastasis*. *Mol Cell Proteomics*, 2012. **11**(7): p. M112 017558.
121. Reddy, B.V. and R.D. Kalraiya, *Sialilated beta1,6 branched N-oligosaccharides modulate adhesion, chemotaxis and motility of melanoma cells: Effect on invasion and spontaneous metastasis properties*. *Biochim Biophys Acta*, 2006. **1760**(9): p. 1393-402.
122. Christie, D.R., et al., *ST6Gal-I expression in ovarian cancer cells promotes an invasive phenotype by altering integrin glycosylation and function*. *J Ovarian Res*, 2008. **1**(1): p. 3.
123. Uemura, T., et al., *Contribution of sialidase NEU1 to suppression of metastasis of human colon cancer cells through desialylation of integrin beta4*. *Oncogene*, 2009. **28**(9): p. 1218-29.
124. Lee, M., et al., *Sialylation of integrin beta1 is involved in radiation-induced adhesion and migration in human colon cancer cells*. *Int J Radiat Oncol Biol Phys*, 2010. **76**(5): p. 1528-36.

125. Kremser, M.E., et al., *Characterisation of alpha3beta1 and alpha(v)beta3 integrin N-oligosaccharides in metastatic melanoma WM9 and WM239 cell lines*. Biochim Biophys Acta, 2008. **1780**(12): p. 1421-31.
126. Lin, S., et al., *Cell surface alpha 2,6 sialylation affects adhesion of breast carcinoma cells*. Exp Cell Res, 2002. **276**(1): p. 101-10.
127. Rae, J.M., et al., *MDA-MB-435 cells are derived from M14 melanoma cells--a loss for breast cancer, but a boon for melanoma research*. Breast Cancer Res Treat, 2007. **104**(1): p. 13-9.
128. Lee, S.H., et al., *Regulation of ionizing radiation-induced adhesion of breast cancer cells to fibronectin by alpha5beta1 integrin*. Radiat Res, 2014. **181**(6): p. 650-8.
129. Semel, A.C., et al., *Hyposialylation of integrins stimulates the activity of myeloid fibronectin receptors*. J Biol Chem, 2002. **277**(36): p. 32830-6.
130. Pretzlaff, R.K., V.W. Xue, and M.E. Rowin, *Sialidase treatment exposes the beta1-integrin active ligand binding site on HL60 cells and increases binding to fibronectin*. Cell Adhes Commun, 2000. **7**(6): p. 491-500.
131. Gu, J. and N. Taniguchi, *Potential of N-glycan in cell adhesion and migration as either a positive or negative regulator*. Cell Adh Migr, 2008. **2**(4): p. 243-5.
132. Lawrence, M.B. and T.A. Springer, *Leukocytes roll on a selectin at physiologic flow rates: distinction from and prerequisite for adhesion through integrins*. Cell, 1991. **65**(5): p. 859-73.

133. Yamamoto, H., et al., *Alpha2,6-sialylation of cell-surface N-glycans inhibits glioma formation in vivo*. *Cancer Res*, 2001. **61**(18): p. 6822-9.
134. Yamamoto, H., et al., *alpha2,6-Sialyltransferase gene transfection into a human glioma cell line (U373 MG) results in decreased invasivity*. *J Neurochem*, 1997. **68**(6): p. 2566-76.
135. Martin, R.G., et al., *Radiation-related pericarditis*. *Am J Cardiol*, 1975. **35**(2): p. 216-20.
136. Tolba, K.A. and E.N. Deliargyris, *Cardiotoxicity of cancer therapy*. *Cancer Invest*, 1999. **17**(6): p. 408-22.
137. Brand, M.D., et al., *Radiation-associated valvular heart disease in Hodgkin's disease is associated with characteristic thickening and fibrosis of the aortic-mitral curtain*. *J Heart Valve Dis*, 2001. **10**(5): p. 681-5.
138. Ramyar, A., et al., *Severe valvular toxicity and pericarditis early after radiation therapy in a patient treated for Hodgkin's lymphoma*. *Turk J Pediatr*. **52**(4): p. 423-5.
139. Castellino, S.M., et al., *Morbidity and mortality in long-term survivors of Hodgkin lymphoma: a report from the Childhood Cancer Survivor Study*. *Blood*.
140. Gyenes, G., et al., *Long-term cardiac morbidity and mortality in a randomized trial of pre- and postoperative radiation therapy versus surgery alone in primary breast cancer*. *Radiother Oncol*, 1998. **48**(2): p. 185-90.

141. Correa, C.R., et al., *Coronary artery findings after left-sided compared with right-sided radiation treatment for early-stage breast cancer*. J Clin Oncol, 2007. **25**(21): p. 3031-7.
142. Prosnitz, R.G., Y.H. Chen, and L.B. Marks, *Cardiac toxicity following thoracic radiation*. Semin Oncol, 2005. **32**(2 Suppl 3): p. S71-80.
143. Hansson, G.K., *Inflammation, atherosclerosis, and coronary artery disease*. N Engl J Med, 2005. **352**(16): p. 1685-95.
144. Kume, N., M.I. Cybulsky, and M.A. Gimbrone, Jr., *Lysophosphatidylcholine, a component of atherogenic lipoproteins, induces mononuclear leukocyte adhesion molecules in cultured human and rabbit arterial endothelial cells*. J Clin Invest, 1992. **90**(3): p. 1138-44.
145. Lu, X., et al., *The role of integrin-mediated cell adhesion in atherosclerosis: pathophysiology and clinical opportunities*. Curr Pharm Des, 2008. **14**(22): p. 2140-58.
146. Meerschaert, J. and M.B. Furie, *The adhesion molecules used by monocytes for migration across endothelium include CD11a/CD18, CD11b/CD18, and VLA-4 on monocytes and ICAM-1, VCAM-1, and other ligands on endothelium*. J Immunol, 1995. **154**(8): p. 4099-112.
147. Rosen, H., *Role of CR3 in induced myelomonocytic recruitment: insights from in vivo monoclonal antibody studies in the mouse*. J Leukoc Biol, 1990. **48**(5): p. 465-9.

148. Ley, K., et al., *Getting to the site of inflammation: the leukocyte adhesion cascade updated*. Nat Rev Immunol, 2007. **7**(9): p. 678-89.
149. Cybulsky, M.I., et al., *A major role for VCAM-1, but not ICAM-1, in early atherosclerosis*. J Clin Invest, 2001. **107**(10): p. 1255-62.
150. Libby, P., *Changing concepts of atherogenesis*. J Intern Med, 2000. **247**(3): p. 349-58.
151. Patel, S.S., et al., *Inhibition of alpha4 integrin and ICAM-1 markedly attenuate macrophage homing to atherosclerotic plaques in ApoE-deficient mice*. Circulation, 1998. **97**(1): p. 75-81.
152. Hickey, M.J., D.N. Granger, and P. Kubes, *Molecular mechanisms underlying IL-4-induced leukocyte recruitment in vivo: a critical role for the alpha 4 integrin*. J Immunol, 1999. **163**(6): p. 3441-8.
153. Shih, P.T., et al., *Blocking very late antigen-4 integrin decreases leukocyte entry and fatty streak formation in mice fed an atherogenic diet*. Circ Res, 1999. **84**(3): p. 345-51.
154. Huo, Y., et al., *The chemokine KC, but not monocyte chemoattractant protein-1, triggers monocyte arrest on early atherosclerotic endothelium*. J Clin Invest, 2001. **108**(9): p. 1307-14.
155. Hallahan, D., J. Kuchibhotla, and C. Wyble, *Cell adhesion molecules mediate radiation-induced leukocyte adhesion to the vascular endothelium*. Cancer Res, 1996. **56**(22): p. 5150-5.

156. Quarmby, S., R.D. Hunter, and S. Kumar, *Irradiation induced expression of CD31, ICAM-1 and VCAM-1 in human microvascular endothelial cells*. *Anticancer Res*, 2000. **20**(5B): p. 3375-81.
157. Heckmann, M., et al., *Vascular activation of adhesion molecule mRNA and cell surface expression by ionizing radiation*. *Exp Cell Res*, 1998. **238**(1): p. 148-54.
158. Jahroudi, N., A.M. Ardekani, and J.S. Greenberger, *Ionizing irradiation increases transcription of the von Willebrand factor gene in endothelial cells*. *Blood*, 1996. **88**(10): p. 3801-14.
159. Burdick, M.M., et al., *HCELL is the major E- and L-selectin ligand expressed on LS174T colon carcinoma cells*. *J Biol Chem*, 2006. **281**(20): p. 13899-905.
160. Jones, D.A., C.W. Smith, and L.V. McIntire, *Leucocyte adhesion under flow conditions: principles important in tissue engineering*. *Biomaterials*, 1996. **17**(3): p. 337-47.
161. Gong, Y., L. Hu, and D. Wu, *Effect of ⁶⁰Co gamma-irradiation on the nonspecific cytotoxicity of alveolar macrophages in vitro*. *Environ Health Perspect*, 1992. **97**: p. 167-70.
162. Riley, P.A., *Free radicals in biology: oxidative stress and the effects of ionizing radiation*. *Int J Radiat Biol*, 1994. **65**(1): p. 27-33.

163. Stewart, F.A., S. Hoving, and N.S. Russell, *Vascular Damage as an Underlying Mechanism of Cardiac and Cerebral Toxicity in Irradiated Cancer Patients*. Radiat Res.
164. Kiyohara, H., et al., *Radiation-induced ICAM-1 expression via TGF-beta1 pathway on human umbilical vein endothelial cells; comparison between X-ray and carbon-ion beam irradiation*. J Radiat Res. **52**(3): p. 287-92.
165. Wu, K.L., et al., *Role of intercellular adhesion molecule-1 in radiation-induced brain injury*. Int J Radiat Oncol Biol Phys. **76**(1): p. 220-8.
166. Ning, S., et al., *Targeting integrins and PI3K/Akt-mediated signal transduction pathways enhances radiation-induced anti-angiogenesis*. Radiat Res, 2007. **168**(1): p. 125-33.
167. Pons, I., et al., *Consequences of gamma-irradiation on inflammatory cytokine regulation in human monocytes/macrophages*. Int J Radiat Biol, 1997. **71**(2): p. 157-66.
168. Kawana, A., et al., *Expression of intercellular adhesion molecule-1 and lymphocyte function-associated antigen-1 on alveolar macrophages in the acute stage of radiation-induced lung injury in rats*. Radiat Res, 1997. **147**(4): p. 431-6.
169. Chigaev, A., et al., *Regulation of cell adhesion by affinity and conformational unbending of alpha4beta1 integrin*. J Immunol, 2007. **178**(11): p. 6828-39.

170. Hynes, R.O., *Integrins: versatility, modulation, and signaling in cell adhesion*. Cell, 1992. **69**(1): p. 11-25.
171. Guerrero-Esteo, M., et al., *Role of two conserved glycine residues in the beta-propeller domain of the integrin alpha4 subunit in VLA-4 conformation and function*. FEBS Lett, 1998. **429**(1): p. 123-8.
172. Pujades, C., et al., *Integrin alpha 4 cysteines 278 and 717 modulate VLA-4 ligand binding and also contribute to alpha 4/180 formation*. Biochem J, 1996. **313 (Pt 3)**: p. 899-908.
173. Munoz, M., et al., *A novel region of the alpha4 integrin subunit with a modulatory role in VLA-4-mediated cell adhesion to fibronectin*. Biochem J, 1997. **327 (Pt 3)**: p. 727-33.
174. Prabhakarpanthian, B., et al., *Expression and functional significance of adhesion molecules on cultured endothelial cells in response to ionizing radiation*. Microcirculation, 2001. **8**(5): p. 355-64.
175. Liu, S.Y., et al., *Ligand binding of leukocyte integrin very late antigen-4 involves exposure of sulfhydryl groups and is subject to redox modulation*. Eur J Immunol, 2008. **38**(2): p. 410-23.
176. Kastan, M.B., et al., *A mammalian cell cycle checkpoint pathway utilizing p53 and GADD45 is defective in ataxia-telangiectasia*. Cell, 1992. **71**(4): p. 587-97.

177. Khanna, K.K. and M.F. Lavin, *Ionizing radiation and UV induction of p53 protein by different pathways in ataxia-telangiectasia cells*. *Oncogene*, 1993. **8**(12): p. 3307-12.
178. Falck, J., et al., *The ATM-Chk2-Cdc25A checkpoint pathway guards against radioresistant DNA synthesis*. *Nature*, 2001. **410**(6830): p. 842-7.
179. Beamish, H. and M.F. Lavin, *Radiosensitivity in ataxia-telangiectasia: anomalies in radiation-induced cell cycle delay*. *Int J Radiat Biol*, 1994. **65**(2): p. 175-84.
180. Santivasi, W.L. and F. Xia, *Ionizing radiation-induced DNA damage, response, and repair*. *Antioxid Redox Signal*, 2014. **21**(2): p. 251-9.
181. Norbury, C.J. and B. Zhivotovsky, *DNA damage-induced apoptosis*. *Oncogene*, 2004. **23**(16): p. 2797-808.
182. Walter, P. and D. Ron, *The unfolded protein response: from stress pathway to homeostatic regulation*. *Science*, 2011. **334**(6059): p. 1081-6.
183. Schwarz, D.S. and M.D. Blower, *The endoplasmic reticulum: structure, function and response to cellular signaling*. *Cell Mol Life Sci*, 2016. **73**(1): p. 79-94.
184. Dufey, E., et al., *Cellular mechanisms of endoplasmic reticulum stress signaling in health and disease. 1. An overview*. *Am J Physiol Cell Physiol*, 2014. **307**(7): p. C582-94.

185. Harding, H.P., et al., *Transcriptional and translational control in the Mammalian unfolded protein response*. *Annu Rev Cell Dev Biol*, 2002. **18**: p. 575-99.
186. Joshi, M., A. Kulkarni, and J.K. Pal, *Small molecule modulators of eukaryotic initiation factor 2alpha kinases, the key regulators of protein synthesis*. *Biochimie*, 2013. **95**(11): p. 1980-90.
187. Kim, E.J., et al., *Ionizing radiation activates PERK/eIF2alpha/ATF4 signaling via ER stress-independent pathway in human vascular endothelial cells*. *Int J Radiat Biol*, 2014. **90**(4): p. 306-12.
188. Kim, K.W., et al., *Endoplasmic reticulum stress mediates radiation-induced autophagy by perk-eIF2alpha in caspase-3/7-deficient cells*. *Oncogene*, 2010. **29**(22): p. 3241-51.
189. Moretti, L., et al., *Switch between apoptosis and autophagy: radiation-induced endoplasmic reticulum stress?* *Cell Cycle*, 2007. **6**(7): p. 793-8.
190. Chiu, H.W., et al., *Monascuspiloin enhances the radiation sensitivity of human prostate cancer cells by stimulating endoplasmic reticulum stress and inducing autophagy*. *PLoS One*, 2012. **7**(7): p. e40462.
191. Yamamori, T., et al., *ER stress suppresses DNA double-strand break repair and sensitizes tumor cells to ionizing radiation by stimulating proteasomal degradation of Rad51*. *FEBS Lett*, 2013. **587**(20): p. 3348-53.

192. Brewer, J.W. and J.A. Diehl, *PERK mediates cell-cycle exit during the mammalian unfolded protein response*. Proc Natl Acad Sci U S A, 2000. **97**(23): p. 12625-30.
193. Hamanaka, R.B., et al., *PERK and GCN2 contribute to eIF2alpha phosphorylation and cell cycle arrest after activation of the unfolded protein response pathway*. Mol Biol Cell, 2005. **16**(12): p. 5493-501.
194. Zhang, F., et al., *Ribosomal stress couples the unfolded protein response to p53-dependent cell cycle arrest*. J Biol Chem, 2006. **281**(40): p. 30036-45.
195. Wang, Z., et al., *Cyclin B1/Cdk1 coordinates mitochondrial respiration for cell-cycle G2/M progression*. Dev Cell, 2014. **29**(2): p. 217-32.
196. Jin, P., Y. Gu, and D.O. Morgan, *Role of inhibitory CDC2 phosphorylation in radiation-induced G2 arrest in human cells*. J Cell Biol, 1996. **134**(4): p. 963-70.
197. Rosner, M., K. Schipany, and M. Hengstschlager, *Merging high-quality biochemical fractionation with a refined flow cytometry approach to monitor nucleocytoplasmic protein expression throughout the unperturbed mammalian cell cycle*. Nat Protoc, 2013. **8**(3): p. 602-26.
198. Momcilovic, O., et al., *Ionizing radiation induces ataxia telangiectasia mutated-dependent checkpoint signaling and G(2) but not G(1) cell cycle arrest in pluripotent human embryonic stem cells*. Stem Cells, 2009. **27**(8): p. 1822-35.

199. Hickson, I., et al., *Identification and characterization of a novel and specific inhibitor of the ataxia-telangiectasia mutated kinase ATM*. *Cancer Res*, 2004. **64**(24): p. 9152-9.
200. Thomas, S.E., et al., *p53 and translation attenuation regulate distinct cell cycle checkpoints during endoplasmic reticulum (ER) stress*. *J Biol Chem*, 2013. **288**(11): p. 7606-17.
201. Tian, H., et al., *Radiation-induced phosphorylation of Chk1 at S345 is associated with p53-dependent cell cycle arrest pathways*. *Neoplasia*, 2002. **4**(2): p. 171-80.
202. Morgan, M.A. and T.S. Lawrence, *Molecular Pathways: Overcoming Radiation Resistance by Targeting DNA Damage Response Pathways*. *Clin Cancer Res*, 2015. **21**(13): p. 2898-904.
203. Kastan, M.B. and D.S. Lim, *The many substrates and functions of ATM*. *Nat Rev Mol Cell Biol*, 2000. **1**(3): p. 179-86.
204. Zhang, T., et al., *The ATM inhibitor KU55933 sensitizes radioresistant bladder cancer cells with DAB2IP gene defect*. *Int J Radiat Biol*, 2015. **91**(4): p. 368-78.
205. Toulany, M., et al., *Cisplatin-mediated radiosensitization of non-small cell lung cancer cells is stimulated by ATM inhibition*. *Radiother Oncol*, 2014. **111**(2): p. 228-36.
206. Carruthers, R., et al., *Abrogation of radioresistance in glioblastoma stem-like cells by inhibition of ATM kinase*. *Mol Oncol*, 2015. **9**(1): p. 192-203.

207. Xu, B., et al., *Two molecularly distinct G(2)/M checkpoints are induced by ionizing irradiation*. Mol Cell Biol, 2002. **22**(4): p. 1049-59.
208. Wu, D., et al., *ERK activity facilitates activation of the S-phase DNA damage checkpoint by modulating ATR function*. Oncogene, 2006. **25**(8): p. 1153-64.
209. Alvino, G.M., et al., *Replication in hydroxyurea: it's a matter of time*. Mol Cell Biol, 2007. **27**(18): p. 6396-406.
210. de Feraudy, S., et al., *Pol eta is required for DNA replication during nucleotide deprivation by hydroxyurea*. Oncogene, 2007. **26**(39): p. 5713-21.
211. Alexandrou, A.T. and J.J. Li, *Cell cycle regulators guide mitochondrial activity in radiation-induced adaptive response*. Antioxid Redox Signal, 2014. **20**(9): p. 1463-80.
212. Arakaki, N., et al., *Dynamics of mitochondria during the cell cycle*. Biol Pharm Bull, 2006. **29**(9): p. 1962-5.
213. Mitra, K., et al., *A hyperfused mitochondrial state achieved at G1-S regulates cyclin E buildup and entry into S phase*. Proc Natl Acad Sci U S A, 2009. **106**(29): p. 11960-5.
214. Mandal, S., et al., *Mitochondrial regulation of cell cycle progression during development as revealed by the tenured mutation in Drosophila*. Dev Cell, 2005. **9**(6): p. 843-54.

215. Candas, D., et al., *CyclinB1/Cdk1 phosphorylates mitochondrial antioxidant MnSOD in cell adaptive response to radiation stress*. J Mol Cell Biol, 2013. **5**(3): p. 166-75.



OHIO
UNIVERSITY

Thesis and Dissertation Services